JRC Scientific and Technical Reports

Displacement Based Design Methodologies for Bridges

LESSLOSS Project / Sub-Project 8: JRC Final Report Contribution

Carlo PAULOTTO, Gustavo AYALA, Fabio TAUCER

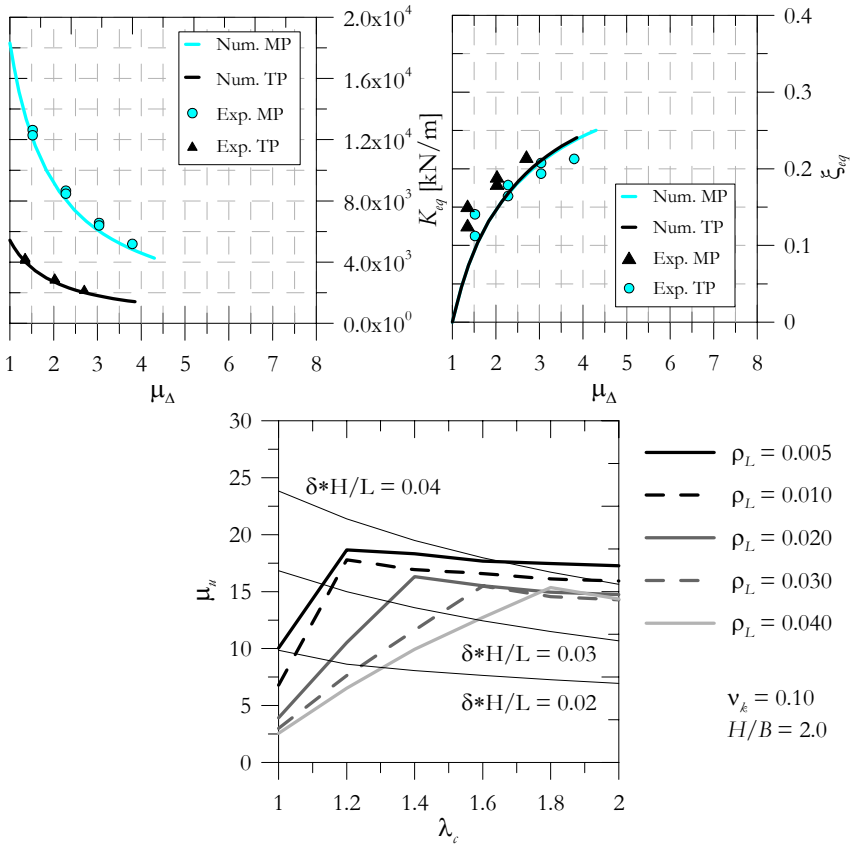

EUR 22894 EN - 2007

JRC EUROPEAN COMMISSION

ipsc Institute for the Protection and Security of the Citizen

lessloss

The Institute for the Protection and Security of the Citizen provides researchbased, systems-oriented support to EU policies so as to protect the citizen against economic and technological risk. The Institute maintains and develops its expertise and networks in information, communication, space and engineering technologies in support of its mission. The strong crossfertilisation between its nuclear and non-nuclear activities strengthens the expertise it can bring to the benefit of customers in both domains.

European Commission
Joint Research Centre
Institute for the Protection and Security of the Citizen

Contact information
Address: Fabio TAUCER
E-mail: fabio.taucer@jrc.it
Tel.: +39 0332 78.5886
Fax: +39 0332 78.9049

http://ipsc.jrc.ec.europa.eu
http://www.jrc.ec.europa.eu

JRC38080

EUR 22894 EN
ISSN 1018-5593

Luxembourg: Office for Official Publications of the European Communities

Printed in Italy

Displacement Based Design Methodologies for Bridges

EXECUTIVE SUMMARY

This report is the result of the contribution of the JRC towards the LESSLOSS Final Report on "Guidelines for Displacement-based Design of Buildings and Bridges", edited by M. N. Fardis and printed by the IUSS Press of the Istituto Universitario Superiore di Pavia.

The report is divided into three sections. The first section addresses the problem of the Displacement Based Evaluation/Design (DBE/D) of reinforced concrete bridges, focusing on the aims and limitations of current seismic evaluation and design practice and the tendencies of the displacement-based seismic evaluation/design methods. It presents a state-of-the-art review on the most important results and lessons derived from previous works, and based on them, two evaluation/design methods consistent with the performance-based seismic design philosophy are presented.

The second section presents the secant stiffness and equivalent viscous damping properties of reinforced concrete hollow rectangular bridge piers, both evaluated at maximum pier displacement, representing a significant design tool of direct application to the DBD of bridges, based on the concept of a substitute linear structure as originally defined by Gulkan and Sozen in 1967s.

The third section addresses how to determine the deformability or stiffness of bridge piers resulting from the relative contributions of flexural and shear deformations, thus complementing the information given in the first two sections, necessary to complete the performance based design and assessment of a bridge.

TABLE OF CONTENTS

LIST OF TABLES

LIST OF FIGURES

1. EVALUATION OF ITERATIVE DBD PROCEDURES FOR BRIDGE

During the last decade, research activities in earthquake engineering have witnessed an increasing pressure from owners, insurance companies, politicians and engineers to re-evaluate and improve the state of practice of seismic design to meet the challenge of reducing life losses and the huge economic impact attributed to recent earthquakes, which by no means could be considered as unusual or rare. As a result of this pressure, different research groups have reinitiated the investigations on the concepts and procedures for the performance based seismic evaluation and design of structures.

This section presents an evaluation of the different methodologies proposed to date to obtain, in a simplified manner, the performance of a structure for the assessment of existent bridges and for the design of new ones, and proposes a set of improvements to guarantee their validity for successful application in practice.

Based on previous work developed by the authors, the premise of this investigation is that regardless of the approximations involved in the different methods considered, the approach used for the evaluation and the design of structures should be only one, which, for the evaluation process considers as known the design of the structure and the seismic demand for which it needs to be evaluated, and as unknown the performance of the structure under design actions, while for the design process considers as known the target performance levels and the seismic demand and, as unknown the design parameters which guarantee such performance levels. With this premise in mind, a critical review of a particular class of approximate linear and non-linear evaluation/design methods based on displacements is carried out, and new alternatives which correct some of the deficiencies of the methods currently used are proposed.

Two methods are considered in this investigation, which have as theoretical foundation the concepts of structural dynamics approximated to systems with non-linear behaviour. In the first method considered, the original structure is substituted by a reference linear elastic structure with elements with reduced stiffness and energy dissipation characteristics consequent with the obtained/expected performance levels. This method, iterative in nature, involves the reduction of a substitute structure (see Section 1.2) to an, incorrectly termed, "equivalent" SDOF system from which performance, the evaluation or the design conditions for the complete structure may be found. The second method, also iterative, is non-linear in nature and considers as basic assumption that the performance of the complete structure, generally expressed in terms of a modal index, *e.g.*, modal ductility, may be approximately transformed to a local ductility, and that the non-linear performance of the structure may be approximately related to that of a reference non-linear SDOF system with a response curve directly derived from the non-linear capacity of the structure.

To validate the correctness and illustrate the application of both methods, six different bridges, considering regular and irregular cases, are evaluated. The results obtained show that under certain circumstances, both approximate methods fail to give acceptable results, suggesting that there exists a regularity condition, not only related to geometric considerations but also to more general structural and seismic demand characteristics, for which the results from the evaluation or design process may be erroneous. The work done has tried with limited success to eliminate this drawback; nevertheless this problem, still under investigation, persists.

1.1 STATE-OF-THE-ART

Since the beginning of the last decade it has been recognized by authors like Moehle [1992] and Priestley [1993] that current methodologies of earthquake resistant design of structures based on forces and strengths do not agree with the seismic performance observed in real reinforced concrete structures, and that it would be much better to use design methodologies based directly on displacements and deformations and/or other valid seismic performance indices. In accordance with this position, in recent years there have been significant advances in the development of design procedures based on performance having as main objective their incorporation in future design codes. In this context, Moehle [1992] proposed a general framework for earthquake resistant design of structures based on drift displacements with the seismic demand given by displacement response spectra.

The procedure for the displacement based design of SDOF systems or systems which may be reduced to "equivalent" linear SDOF systems, such as those proposed by Priestley [1993], Kowalsky *et al* [1995], Priestley [2000] and Kowalsky [2002], starts from a target design displacement, based on a deformation capacity guaranteed by an appropriate detailing of the structure. Assuming that reasonable values for the yielding displacements may be assumed from the geometry of the elements, displacement ductility demands may be directly calculated from target peak displacements. Starting with these ductilities and with a set of response displacement spectra, the effective period of an equivalent linear viscoelastic SDOF system is determined at peak displacement, considering an equivalent damping ratio which includes the inherent viscous damping characteristics of the structure and that required to consider the energy dissipated by the system through non-linear hysteretic behaviour. The final result of this process is the required yielding strength determined from the peak displacement and the secant stiffness corresponding to the effective period. Calvi and Kingsley [1995] extended this methodology to Multiple Degree Of Freedom (MDOF) structures which may be transformed to an equivalent SDOF system using an assumed deformed configuration of the structure. For buildings it is proposed that the assumed deformed configuration is that corresponding to a predefined plastic mechanism. The final result of this alternative is the required strength that should be given to the structure to attain the objective performance. An alternative evaluation method described in documents such as FEMA-273 [FEMA, 1997] is based on an elastic approximation of maximum displacements multiplied by a set of modification factors to arrive at an estimate of the target inelastic displacement.

An alternative approach to the performance based evaluation/design of structures is based on the use of approximate non-linear static analysis procedures (pushover like analyses) to include, in a simple method, the most important features which influence performance [Freeman, 1978], [Fajfar, 1999]. Examples of the methods which use a single mode approximation are described in documents such as the ATC-40 [ATC, 1996] and Eurocode 8 [CEN, 2003].

An improvement of the single mode approximation is to include the contribution of higher modes into the forces used for pushover. Relevant formulations of this multimode approximation are in De Rue [1998], Requena and Ayala [2000] and Gupta and Kunnath [2000]. Even though the application of modal spectrum analysis in the inelastic domain to define the distribution of lateral forces used to determine the capacity curve of the structure is theoretically incorrect, the reported results from this approach show an acceptable approximation.

Two more recent approximate methods based on the combination of modal responses are the modal pushover analysis originally preposed by Paret *et al.* [1996] and later on improved and successfully used by Chopra and Goel [2002] and the Incremental Response Spectrum Analysis (IRSA) proposed by Aydinoğlu [2003]. In the first method, pushover analyses are independently carried out separately for each participating mode and the performance of the structure is obtained by adding the modal contributions using a modal combination rule. All the important

modes, identified in the initial - elastic state, are used separately to determine the distribution of forces for the pushover analyses, *i.e.,* the number of analyses is equal to the number of important modes in the elastic state.

The IRSA method was originally developed as an approximated step-by-step piecewise dynamic modal analysis for non-linear structures and then conveniently simplified for practical applications using smooth response spectrum [Aydinoğlu, 2003]. The method takes into account the influence of all important modes and the changes in the dynamic properties of the structure every time a plastic hinge occurs. Modal capacity diagrams for each important mode are constructed through modal analyses. To calculate the performance of the structure the procedure uses a modal combination rule with previously scaled modal responses according to some "inter-modal scale factors". In the practical version of the method these factors are simplified as constant each time a sequential modal spectrum analysis is carried out. In the method, once the modal capacity curves are defined, the modal performance of the structure is obtained by using, for each mode, the equal displacement rule with the consideration of the short period correction. To obtain the global performance of the structure an accepted modal combination rule is used. This method is different to pushover-based procedures as equivalent static forces are never applied to construct the modal capacity diagrams. Instead, the method uses displacements derived from consecutive modal analysis to obtain the different segments of the modal capacity diagrams corresponding to different performance stages.

1.2 METHOD BASED ON THE SUBSTITUTE STRUCTURE

One of the mostly used methods for the displacement based evaluation/design of bridges is one in which the original structure is substituted by a linear viscoelastic counterpart, *e.g*, Kowalsky [2002]. This "substitute" structure has the same configuration as the original, with equivalent stiffness and damping properties assigned to the elements where damage actually occurs or it is assumed to occur, when performing evaluation and design applications, respectively.

The concept of introducing viscous damping to represent energy dissipation characteristics of a system was first presented by Jacobsen [1960]. However, the first known earthquake engineering application of this idea to approximately substitute a hysteretic SDOF system subjected to earthquake action by a viscoelastic one was investigated by Rosenblueth and Herrera [1964].

For the assessment of real structures, Gulkan and Sozen [1974] introduced formally the concept of substitute structure for a SDOF structure comparing the resulting analytical results with the corresponding experimental ones. Later on, Shibata and Sozen [1976] extended this formulation to MDOF systems by proposing an approximation to define the modal damping ratio of the whole structure as a weighted average of the element damping ratios. In this approximation, once the equivalent linear stiffness of the elements and the modal damping ratio of the structure are determined, modal spectral analysis may be used to approximately evaluate its seismic performance.

Recent papers by Blandon and Priestley [2005] and Dwairi [2004], Guyader and Iwan [2006], among other authors, present a thorough list of different definitions of equivalent viscous damping, ξ_{eq}, and where applicable, effective periods, T_{eff}. In this section all proposed definitions are not presented, referring the reader to Ayala *et al.* [2007].

1.2.1 The substitute structure applied to the displacement based evaluation of bridges

In this section it is assumed that for evaluation purposes the bridge structure under consideration is already designed and that the substitute structure method is used to assess its seismic

performance when subjected to a seismic demand given by a design spectrum. The steps involved are illustrated in Figure 1.1 and are:

Step-1: Determination of the inelastic behaviour of the pier sections, as moment *vs.* curvature, within the potential damaged region when subjected to increasing cyclic curvature.

Step-2: Determination of the load-displacement characteristics at the top of the piers. Based on the moment *vs.* curvature curves determined in step 1 and on an assumption for the length of the plastic hinge, load-displacement curves for the top of the piers, considering the different maximum lateral displacement (ductility) levels, are constructed.

Step-3: Determination of equivalent linear viscoelastic properties of the piers. Based on the nonlinear force *vs.* displacement curves of the piers determined in step 2, the equivalent linear viscoelastic properties of the piers, *e.g.,* secant stiffness, K_{eff}, and equivalent viscous damping ratio, ξ_{eq}, at maximum displacement, are calculated. A procedure to find the properties determined in steps 1 through 3 is proposed and exemplified in Section 2.

Step-4: Construction of the curves for each pier depicting the variation of the equivalent stiffness and damping ratio in terms of displacement ductility. To consider the transient nature of the earthquake action in the equivalent properties curves, it is necessary to include a modification factor that takes into account the fact that the maximum displacement attained during an earthquake occurs only a very limited number of times, *e.g.*, for narrow band records, equivalent properties associated to the maximum displacement multiplied by a factor equal to 0.67 have shown to be a good approximation.

Step-5: Initiation of the iterative procedure for performance determination. Since the equivalent viscoelastic properties of the piers are functions of the associated maximum displacements, it is required to initially assume a distribution of maximum displacements under design conditions. A simple way to obtain this distribution of maximum displacements is to carry out a modal spectral analysis considering for the piers the initial stiffness and the inherent modal viscous damping for this type of structures.

Step-6: Assumption of the performance of the bridge. The distribution of maximum displacements is made equal, for the first iteration, to the displacements obtained from step 5, and for subsequent iterations, to the displacements obtained from step 8.

Step-7: Determination of the performance of the bridge. Assuming an elastic bridge deck, modal analysis is carried out on the bridge structure, with viscoelastic properties of the piers determined from the equivalent properties curves derived in step 4 at the maximum displacement distribution assumed in step 6. The equivalent modal viscous damping ratios for the bridge can be evaluated for each mode as the sum of the inherent modal damping, ξ_o, and that corresponding to the weighted average of the equivalent hysteretic damping ratios for all the structural elements using the original approach of Shibata and Sozen [1976].

Step-8: Update the performance of the bridge. The distribution of maximum displacements is made equal to the distribution of displacements computed from step 7.

Step-9: Comparison of the updated and the assumed performances. When, during the iteration process, the ratio between the updated (from step 8) and the assumed (from step 6) performances is within an accepted tolerance, the process is stopped and the performance of the bridge equals the displacement distribution from step 8, otherwise steps 6 through 9 are repeated.

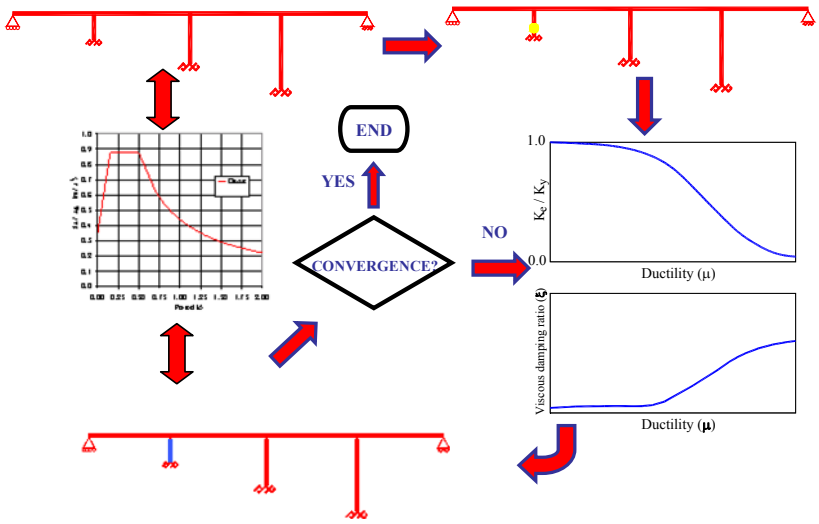

Figure 1.1 Evaluation procedure for the method based on the substitute structure

1.2.2 The substitute structure applied to the displacement based design of bridges

A similar procedure to that described above for evaluation may be used for the DDBD of bridge structures. The design procedure proposed in this chapter is derived following similar steps to those presented in the above section and it is different to that presented by Kowalsky [2002] inasmuch as it includes information about a target damaged distribution under design conditions, includes the participation of all contributing modes and uses as basic design information the relations between the inelastic deformation at the top of the piers *vs.* local curvature demands at the hinges at the base of the damaged piers.

To apply this procedure it is necessary to have, for different pier geometries and acceptable design configurations, design curves similar to those illustrated in Section 2. The procedure is schematically shown in Figure 1.2 and the steps describing its application are described in the following:

Step 1. Perform a conventional force design for permanent plus vehicular plus earthquake loads, choosing an acceptable target design index, *e.g.*, a global ductility factor.

Step 2. Considering an elastic bridge deck and based on the results of step 1, check if the damage distribution, obtained by comparing the maximum displacements at the top of the piers with their corresponding yield displacements, is acceptable, in which case go to step 3, otherwise modify he design of those piers where no damage is accepted to occur or where the ductility demand is not acceptable, and go to step 1.

Step 3. Calculate the additional damping ratios and reduced stiffness for the damaged piers as presented in steps 1 through 4 of Chapter 1.2.1, and perform the seismic analysis of the corresponding substitute structure.

Step 4. Compare the calculated maximum pier displacements with those considered as target in the design. Based on this comparison and on the information presented in Section 2, modify, if required, the design of the piers and calculate the new local ductility demands of the damaged piers and go back to step 3, otherwise go to step 5.

Step 5. The design of the bridge has converged to an acceptable target performance distribution. It is important to mention that if the target performance is not reached, this could be due to the choice of an unfeasible damage distribution, in this case an alternative distribution should be considered.

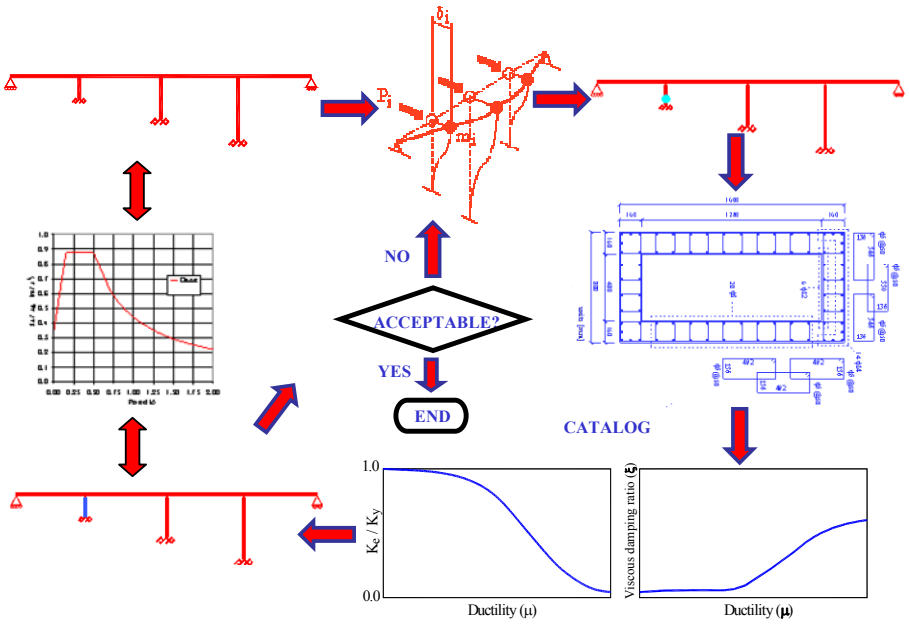

Figure 1.2 Design procedure for the method based on the substitute structure

1.3 METHOD BASED ON THE NON-LINEAR CAPACITY OF THE STRUCTURE

From the detailed study of the existing procedures for evaluation and design of bridges based on the non-linear capacity of structures, it has been found that, in general, all involve the following two tasks:

1. Determination of the deformation capacity of the structure and its corresponding strength for the sequential formation of the events (*e.g.,* plastic hinges) associated to predefined limits states and the corresponding redistribution of the seismic forces which act on the structure.

2. Determination of the seismic performance using displacement/acceleration design spectra; considering SDOF systems (one or several systems, depending on the method) whose non-linear force-displacement relationships are derived from the results of step 1. The use of smooth spectrum produces, for evaluation purposes, the maximum displacement, *i.e.,* the displacement demand for a given design, and for design purposes, the strength demand for a required displacement.

Based on the same concepts which support these two tasks, a performance evaluation/design method is proposed using the same hypotheses and considerations as the method developed by Ayala [2001], which explicitly considers the non-linear behaviour of the structure on the derivation/postulation of a target response curve of a reference SDOF system considering the participation of all modes to determine the performance of the otherwise MDOF of the structure under evaluation/design. The characteristics of the response curve of the reference SDOF system are obtained from the calculated/desired distributions of damage for the considered design objective. In this method, the design seismic demands associated to each of the design objectives are concurrently determined using the characteristics of the calculated/assumed response curve of the reference SDOF.

The evaluation version of this method is an evolution of the procedure proposed by Requena and Ayala [2000]. In this method the maximum displacement of the reference system is obtained from one of the different variations of the equal displacement rule, *e.g.*, Fajfar [1999] and Ruiz-Garcia and Miranda [2004], and directly transformed to the maximum displacement of the structure by an *ad hoc* modal spectral analysis. This method is similar to the IRSA method, however, it differs in the way in which higher modes are considered. The details of the application of this method are presented in Ayala *et al.* [2007].

A key question in the application of displacement-based evaluation/design methods to MDOF structures is how to transform global performance into demands of local inelastic deformation in the individual structural members. In this respect, detailed procedures intended to achieve this purpose are, for example, those proposed by Seneviratna and Krawinkler [1997], however a definite solution to this problem has not been established and it is still the topic of current investigations.

1.3.1 Non-linear capacity concept applied to the displacement based evaluation of bridges

The application of the proposed method involves the following steps, schematically illustrated in Figure 1.3:

Step 1. The seismic demand is defined by a smooth response spectrum corresponding to a chosen seismic demand level.

Step 2. The response curve of the reference SDOF system is obtained through a series of Modal Spectral Analyses (MSA) as outlined in Ayala *et al.* [2007], considering as many damage stages developed by the structure as necessary, until its maximum capacity is reached. The contribution of higher modes of vibration in the response curve is taken into account using a modal combination rule (*e.g.,* SRSS or CQC). In this work, a damage stage is defined every time a plastic hinge is formed at the end section of a pier.

Step 3. For each damage state *j*, the corresponding MSA results are used to calculate the scale factor, $Sf_{(j)}$, at the base of each damaged pier using the equations presented in Ayala *et al.* [2007]. The lowest scale factor corresponds to the pier requiring the lowest seismic demand to yield.

Step 4. The scaled pseudo-acceleration, ΔSa, and the scaled spectral displacement, ΔSd, corresponding to the period of the dominant mode of the structure in the j^{th} damage stage, are defined from the scaled spectrum, using an acceleration *vs.* displacement format, ADRS, which is the same format in which the response curve is defined.

Step 5. The capacity of the structure is reached when a local or global instability occurs, indicating that the construction of the response curve is finished and that the methodology for the evaluation of the spectral displacement may be continued. Otherwise, a new damage stage has to be considered and a new MSA performed for the determination of the next point on the response curve.

Step 6. The inelastic displacement demand, or performance spectral displacement, S_d^*, may be calculated using the equal displacement rule [Veletsos and Newmak, 1966], with proper consideration of the short period correction [Fajfar, 1999], as specified in Annex B of EC 8 [CEN, 2003] or by considering more recent results as those of Ruiz-Garcia and Miranda [2004].

Step 7. When the available capacity of the structure exceeds the demand, a new scale factor, Sf_N, needs to be calculated for the first point ("point *j*") of the response curve where the displacement

is larger than the performance displacement. This is done in accordance with the equations presented in Ayala et al. [2007].

The seismic performance of the bridge for the selected performance parameter, in this case the maximum lateral pier displacement, is finally calculated as the weighted sum of the corresponding parameters of the N modal spectral analyses performed until the target performance displacement is reached.

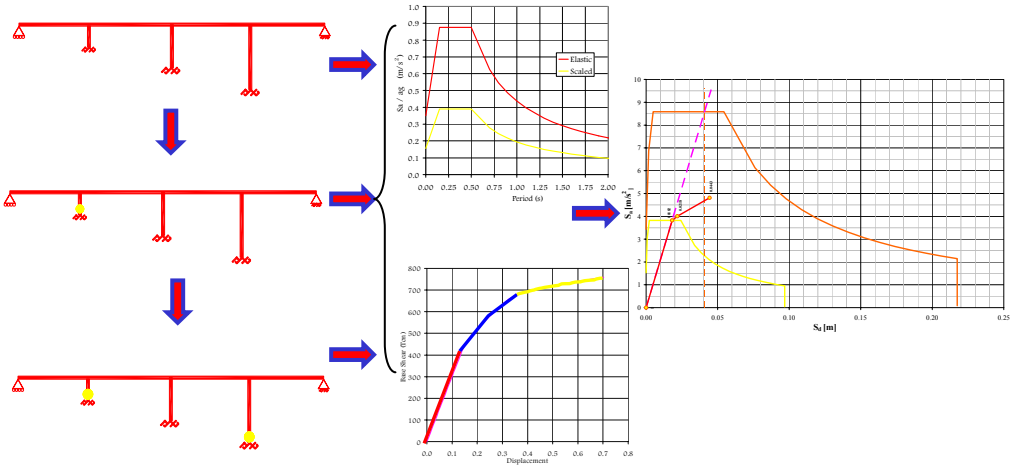

Figure 1.3 Assessment procedure for the proposed method based on the reference structure

1.3.2 Non-linear capacity concept applied to the displacement based design of bridges

The overall process to design a bridge structure to meet a performance level defined by a target design ductility is schematically shown in Figure 1.4 and consists of the following steps:

Step 1. The response curve of a reference system corresponding to the mode of the structure with the highest contribution is constructed by considering two structures with different dynamic properties: one with properties derived from the bridge without damage corresponding to a pre-designed structure; the other, the same bridge with reduced properties to incorporate a proposed damage distribution expected to occur under design demands.

Step 2. The strengths of the bridge piers where damage is accepted to occur are determined from a MSA using the dynamic properties of the undamaged bridge and the elastic design spectrum reduced by a factor defined from the strength spectrum for a system with a global performance index estimated from a design pier displacement. The complementary strengths for the bridge elements where damage is not admitted, corresponding to the second stage, are obtained from a second MSA using the properties of the damaged bridge and the same elastic design spectrum scaled to consider a seismic demand that added to that considered for the first stage gives the total seismic demand.

Step 3. The final design forces are obtained by summing the element forces of the two previously defined MSAs, and combining them with the element forces from the analysis for gravitational and vehicular loads in accordance with the EC8 code or any other valid bridge design code.

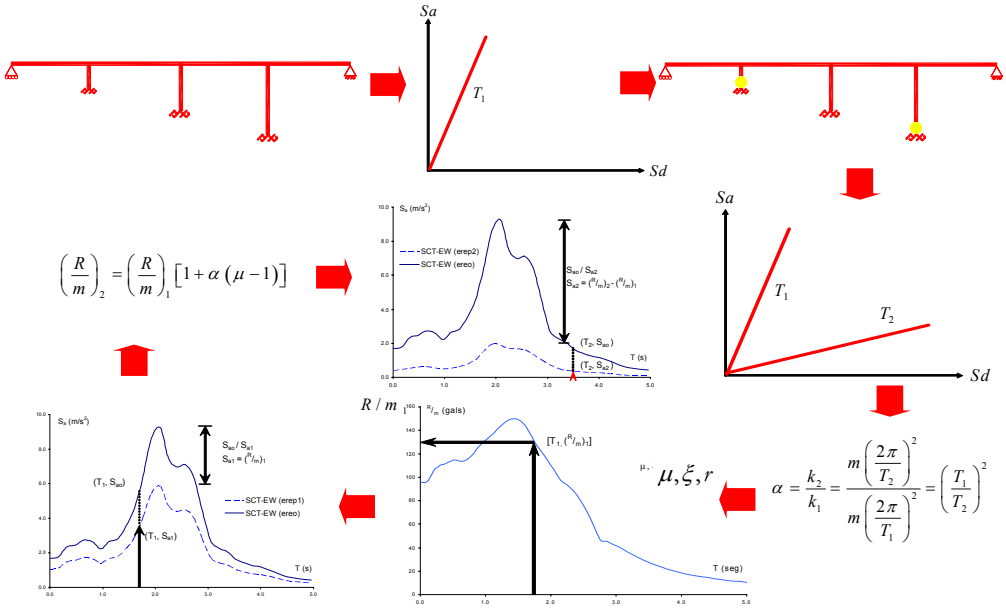

Figure 1.4 Design procedure for the method based on the reference structure

1.4 APPLICATION EXAMPLES

To illustrate the application and validate the accuracy and potentiality of the proposed methods, six sample bridge structures are evaluated. The first structure is a scaled four span single supported concrete bridge tested at ELSA with a variety of pseudo-static and pseudo-dynamic tests [Pinto *et al.*, 1996], while the other five structures have the same configuration as the first, but with different dimensions and characteristics of the piers and superstructure, as designed by Isaković and Fischinger [2006]. The bridges are all reinforced concrete structures designed in accordance with current seismic codes. The general layout of the considered bridges and the geometric and structural characteristics of each bridge are described in Ayala *et al.* [2007]. For all bridges the seismic design level was defined using different intensities of the EC8 design spectrum [CEN, 2003] corresponding to soil type B, 5% damping ratio and a 1.2 soil amplification factor.

The equivalent properties derived for rectangular reinforced concrete hollow piers described in Section 2 were used to construct the substitute structure of the sample bridges analysed. The seismic demands were represented by artificial records compatible with the EC8 design spectrum, with peak accelerations of 0.35g and 0.70g for the ELSA bridge, and peak accelerations ranging from 0.20g to 0.70g for the other five bridges. The calculated performances for all bridge examples considered are described in Ayala *et al.* [2007].

1.5 CONCLUDING REMARKS

This chapter presents two different methods of displacement based evaluation/design of bridges which improve previously developed approximations. The results presented may be directly used to construct a "substitute" structure or a response curve of a reference SDOF system which lead to a sought performance or to a design for a specified design objective defined by a maximum pier displacement and earthquake intensity.

Both proposed methods may be considered enhanced versions of others currently under use or investigation by other research groups, as they take into consideration the contribution of higher modes of vibration and the displacement reversal nature of earthquake action through evolving

modal spectral analyses, rather than from evolving force or displacement based pushover analyses.

The work presented shows that the evaluation and the design options of the proposed methods, may give acceptable results with limited computational effort as long as the structure is "regular". This conclusion unfortunately may not be extended to the case of "irregular" bridges, where the relative relevance to performance of highly correlated modes changes as a function of the earthquake intensity.

It is shown that the use of these methods with response spectra as seismic demand may not guarantee correct results for all seismic design levels consistent with the spectrum, *e.g.,* the results presented in Ayala *et al.* [2007] for the V213P bridge are not satisfactory when compared with those of the statistical study of 1000 non-linear time history analyses. For this example, the observed lack of approximation may be due to the fact that for the considered design level, the bridge, due to the occurrence of new damage, changes its instantaneous fundamental mode shape from rotational to translational, thus becoming irregular. It is evident that more research efforts are needed to fully understand why this lack of approximation occurs, to determine for which combinations of bridge configurations and seismic design levels the application of the proposed methods is reliable.

Preliminary results show that for bridges with a significant contribution of higher modes and with large non-linearities, the methods proposed, in particularly the one based on the non-linear capacity of the structure, lead to better results than alternative simplified procedures based on a "substitute structure" and on an "equivalent" SDOF system, which do not explicitly consider the contribution of higher modes. For the design versions of the methods proposed, the deformation capacity of the structure is obtained from an assumed damage distribution, explicitly defined in the design process.

It is shown that the methods presented may be carried out with commercial analysis software. In particular, for the method based on the non-linear capacity of the structure, the construction of the response curve of the reference system is carried out using partial results of evolving modal spectral analyses. This approach is simpler and superior to others currently used, as it does not depend on results of non-linear pushover analyses with evolving lateral force or displacement distributions. Furthermore, it is accepted that the application of modal spectral analysis with accepted modal combination rules for the evaluation/design of bridges gives results consistent with calculated/expected maximum performances.

2. EQUIVALENT PROPERTIES OF RC RECTANGUAR HOLLOW PIERS

The seismic assessment and design of reinforced concrete bridges requires an accurate description of the stiffness and energy dissipation characteristics of the bridge piers when both refined and simplified methods are used to estimate performance in terms of displacements. The purpose of this chapter is to describe the stiffness and energy dissipation properties of RC bridge piers of rectangular hollow section, for which at present insufficient information is available, based on parametric analyses calibrated against results from experimental tests performed on large-scale specimens.

The Displacement Based Design (DBD) of bridges using simplified methods based on a linearised model of the structure requires the determination of equivalent properties of the nonlinear system. In the following, equivalent properties based on secant stiffness and energy dissipation at maximum displacement are determined for RC rectangular hollow sections. The work involves the use of a continuous non-linear model of the section calibrated against experimental tests, which is used to perform parametric analyses to determine bilinear moment-curvature envelopes and energy dissipation curves in terms of the ductility of the section. The equivalent properties of a generic pier are then derived from the section properties using the plastic hinge approach. A complete description of the procedure and results obtained from the analysis is found in Paulotto *et al.* [2007].

The analysis starts from the identification of the parameters that play a major role in determining the behaviour of the pier sections and their ranges of variation. The following parameters were chosen:

- The section aspect ratio, H/B, where H and B denote the height and width of the section, respectively.
- The mechanical properties of the reinforcing steel and concrete.
- The longitudinal reinforcement ratio:

$$\rho_L = \frac{A_s}{A_c} \tag{2.1}$$

where A_s and A_c are the total areas of longitudinal reinforcement and concrete cross-section.

- The normalized axial force:

$$\nu_k = \frac{N_{Ed}}{A_c \cdot f_{ck}} \tag{2.2}$$

where N_{Ed} is the axial force corresponding to the seismic design condition, A_c is the area of the concrete section and f_{ck} is the characteristic value of the concrete strength.

- The confinement level, defined through Mander's parameter λ_c, as suggested by Annex E of prEN 1998-2 [CEN, 2003].

The range of variation of each of these parameters was determined on the basis of current practice and on prescriptions contained in the Eurocodes, in particular:

- According to prEN 1998-1 7.2.1 (1) [CEN, 2003], the prescribed concrete class in plastic regions should not be lower than C20, and not higher than C40. Concrete classes C25, C30 and C35 were considered.
- According to prEN 1998-1 5.3.2 (1)P [CEN, 2003], class B or C steel reinforcement, as defined in Table C.1 in Normative Annex C of prEN 1992-1-1 [CEN, 2003], should be used in primary seismic elements. Tempcore B500B reinforcing steel, which belongs to class B as defined by Normative Annex C, was considered.
- From a survey of a number of bridge designs it was observed that the thickness of the walls of rectangular hollow sections varies between 0.30 m and 0.50 m. A constant value of 0.40 m was chosen for the wall thickness.
- Longitudinal reinforcement ratios between 0.005 and 0.04 were considered, distributed in two layers as commonly observed in practice. Furthermore, it was assumed that the reinforcement rebars, having all the same size, are uniformly distributed across the section.
- According to design practice, normalized axial force values ranging between 0.10 and 0.40 were considered.
- Values of λ_c ranging between 1.0 and 2.0 were considered.

The values used in the parametric analysis are summarized in Table 2.1 As a result of this preliminary analysis, 2700 possible section designs were considered.

Table 2.1 Values of the parameters used in the analysis of the pier section behaviour

Parameter values	
Wall thickness [m]	0.40
Concrete	C25 C30 C35
H/B	1.0 1.5 2.0 2.5 3.0
steel	Tempcore B500B
ρ_L	0.005 0.010 0.020 0.030 0.040
ν_k	0.10 0.20 0.30 0.40
λ_c	1.0 1.2 1.3 1.4 1.6 1.8 2.0

To obtain the moment-curvature envelope of all the sections considered, nonlinear finite element analyses (using 2D fibre models) with monotonically increasing curvatures were carried out. These envelopes, representing the capacity curves of each section, were approximated with bilinear curves to be used either for evaluation or design purposes. With this aim, the first yield point and the point corresponding to failure were evaluated for each nonlinear envelope curve. The first yield point corresponds to the point on the moment-curvature relationship at which either the first steel fibre reaches the yield strain in tension or the extreme compression fibre attains a strain of 0.002, whichever occurs first. The failure point is reached when either the longitudinal reinforcement or the confined concrete reaches its ultimate strain or when the section strength decreases down to 80% of its maximum value. The confined concrete attains its ultimate compressive strain, according to prEN1998-2 E.2.1 [CEN, 2003], when:

$$\varepsilon_{cu,c} = 0.004 + \frac{1.4 \cdot \rho_s \cdot f_{ym} \cdot \varepsilon_{um}}{f_{cm,c}} \qquad (2.3)$$

where ρ_s is equal to twice the transverse reinforcement ratio, ρ_w, f_{ym} and ε_{um} are the mean values of the yield stress and elongation at maximum stress of the transverse reinforcing steel, respectively, and $f_{cm,c}$ is the mean value of the compressive strength of the confined concrete.

The line that joins the origin and the first yield point gives the initial slope of the bilinear curve; the line that extends through the failure point and balances the areas between the actual and the idealized moment-curvature relationships beyond the first yield point gives the slope of the second branch (see Figure 2.1).

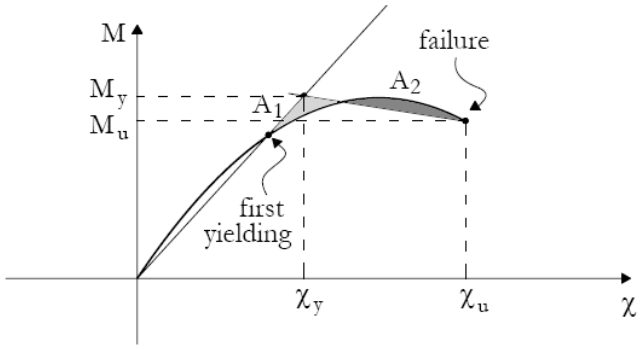

Figure 2.1 Bilinear approximation of the nonlinear envelope curve of the pier section behaviour

Having defined the bilinear moment-curvature relationship, the capacity curve of a generic section may be represented through four parameters: yield curvature and moment, χ_y and M_y, and ultimate curvature and moment, χ_u and M_u, which were used to summarize the results of the parametric analysis in a series of charts [Paulotto *et al.*, 2007]. An example of these charts is shown in Figure 2.2 where the results are expressed in terms of the following dimensionless parameters:

(dimensionless yield curvature) $$\chi_y \cdot H \tag{2.4}$$

(ultimate curvature ductility) $$\mu_u = \frac{\chi_u}{\chi_y} \tag{2.5}$$

(dimensionless yield moment) $$\frac{M_y}{f'_{cm} \cdot B \cdot H^2} \tag{2.6}$$

(post yield stiffness ratio) $$\alpha = \frac{\frac{M_u - M_y}{\chi_u - \chi_y}}{\frac{M_y}{\chi_y}} \tag{2.7}$$

where f'_{cm} is the mean value of the concrete compressive strength defined according to Table 3.1 of prEN 1992-1-1 [CEN, 2003]. By fitting these numerical results, analytical expressions can be determined to estimate the yield curvature and moment for different sections. For example, for sections in which C25 concrete and Tempcore steel rebars are used, the following equations were derived:

$$\chi_y = 0.00552 \cdot \frac{\sqrt{\lambda_c}}{H} \tag{2.8}$$

and

$$\frac{M_y}{f'_{cm} \cdot B \cdot H^2} = 3.66 \cdot \rho_L + 0.159 \cdot \nu_k - 0.00940 \cdot \frac{H}{B} + 0.0227 \qquad (2.9)$$

For the two remaining parameters μ_u and α, it was not possible to derive closed form expression, however, some general considerations regarding their behaviour can be extrapolated (Section 0): μ_u decreases with the increase of H/B, ρ_L and ν_k (for $\lambda_c \leq 1.4$), and α is always lower or equal to 0.01 (*i.e.*, elastoplastic), with the exception of the case when $\lambda_c = 1.0$.

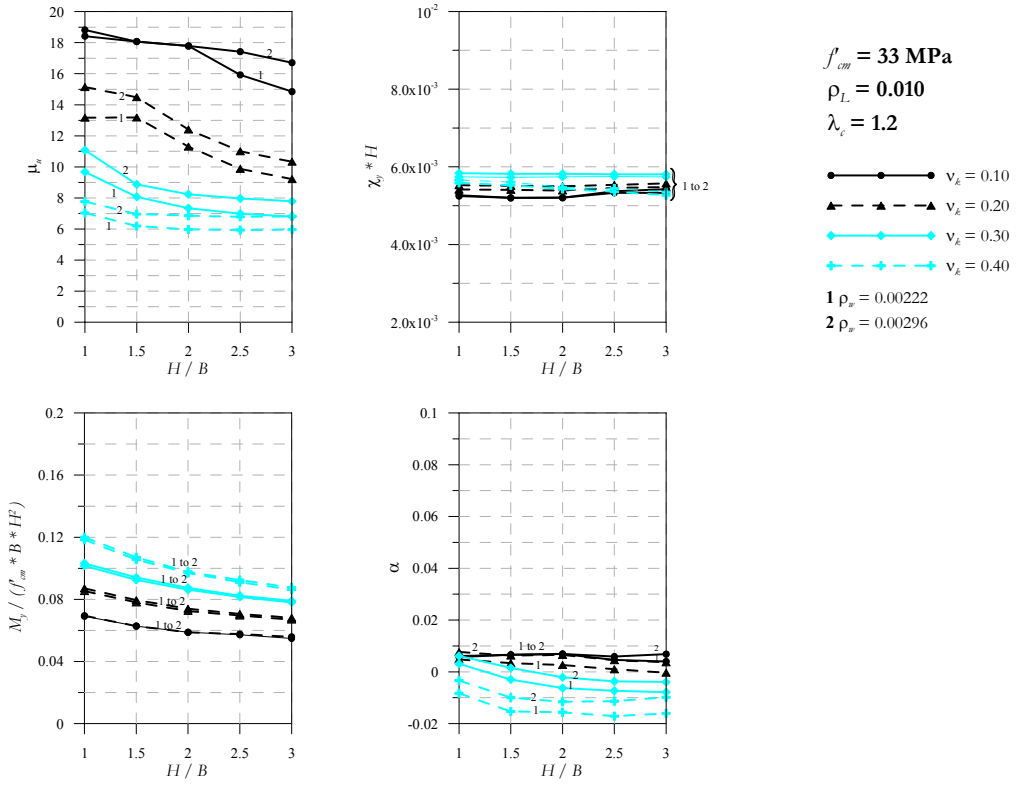

Figure 2.2 Results of the parametric analysis (f'_{cm} = 33 MPa, ρ_L = 0.010, λ_c = 1.2

The hysteretic energy dissipated by the considered sections was evaluated through nonlinear analyses under increasing cyclic curvature, calibrated against experimental results from Pinto *et al.* [1995, 1996]. The results of these analyses are expressed in terms of a dimensionless parameter:

$$\eta = \frac{W}{2 \cdot \pi \cdot M_{\max} \cdot \chi_{\max}} \qquad (2.10)$$

where W is the energy dissipated in one cycle, $M_{\max}$ and $\chi_{\max}$ are the maximum moment and curvature cyclic amplitude, respectively. The results indicate that η does not depend on the section aspect ratio, while it depends strongly on the normalized axial force, although this dependence becomes less strong as the longitudinal reinforcement ratio increases. It was also found that by increasing the confinement of the section, the section ductility increases without any relevant changes in the section strength. Based on this result, all the cyclic analyses were conducted assuming λ_c = 2.0. The results for sections in which C25 concrete and Tempcore steel rebars are used are shown in Figure 2.3, which may be approximated, for $\nu_k \leq 0.30$, by the following equation in terms of ρ_L, ν_k and the current curvature ductility, μ:

$$\eta = \left[1 - \frac{\nu_k - 0.1}{78 \cdot \rho_L}\right] \cdot 0.96 \cdot \rho_L^{0.2} \cdot \left[1 - \frac{1}{\sqrt{\mu}}\right] \qquad (2.11)$$

Using the plastic hinge approach, the properties derived at the section level were used to compute the force-displacement envelope and the energy dissipation characteristics of the piers, which are used to evaluate the pier equivalent properties of stiffness and damping ratio, K_{eq} and ξ_{eq}, respectively.

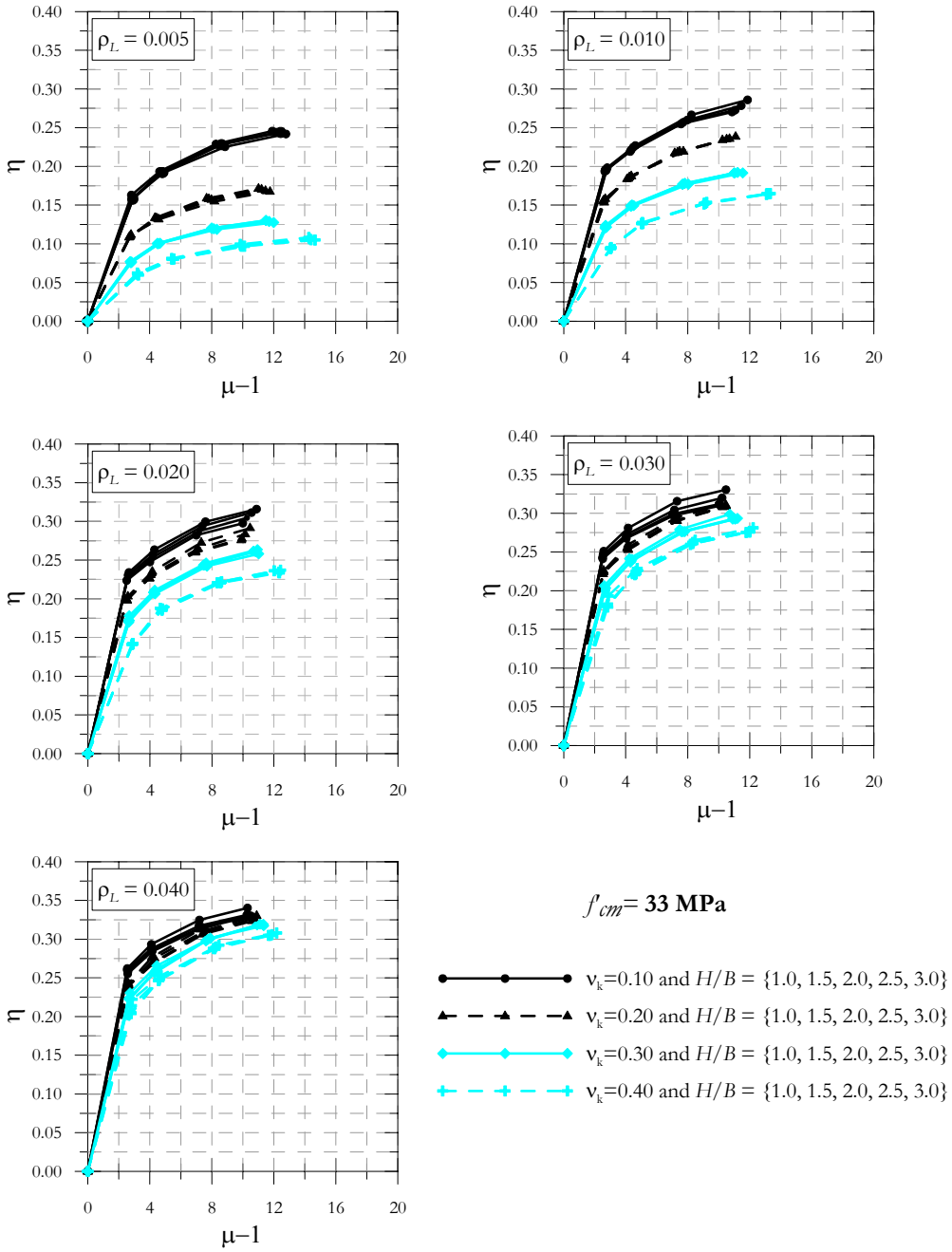

Figure 2.3 Dimensionless energy dissipated by the pier section for cycles with different ductility

The equivalent stiffness of a cantilever pier of height L is defined as the secant stiffness K_{eq} at maximum displacement:

$$\Delta_{\max} = \Delta_y \cdot \mu_\Delta \qquad (2.12)$$

where

$$\Delta_y = \frac{\chi_y \cdot L^2}{3} \tag{2.13}$$

and

$$\mu_\Delta = 1 + (\mu - 1)\left[\alpha + \frac{3L_p}{L}\left(1 - 0.5\frac{L_p}{L}\right)\right] \tag{2.14}$$

are the yield displacement and the ductility displacement of the pier, respectively, with L_p denoting the plastic hinge length. Considering that the force-displacement envelope of the pier is assumed bilinear, the equivalent stiffness is expressed as:

$$\begin{cases} K_{eq} = K_y & \text{when } \mu_\Delta \le 1 \\ K_{eq} = \dfrac{1 + \alpha_\Delta(\mu_\Delta - 1)}{\mu_\Delta} \cdot K_y & \text{when } \mu_\Delta > 1 \end{cases} \tag{2.15}$$

where

$$K_y = \frac{3 \cdot M_y}{\chi_y \cdot L^3} \tag{2.16}$$

$$\alpha_\Delta = \frac{1}{1 + \dfrac{3L_p}{\alpha L}\left(1 - 0.5\dfrac{L_p}{L}\right)} \tag{2.17}$$

are the secant-to-yield stiffness and the post-yield stiffness ratio of the pier, respectively.

The equivalent damping ratio of the pier ξ_{eq} is calculated according to Jacobsen [1930] as:

$$\xi_{eq} = \frac{W_\Delta}{2 \cdot \pi \cdot E_\Delta} \tag{2.18}$$

where W_Δ is the energy dissipated by the pier, approximated as:

$$W_\Delta = W \cdot L_p \tag{2.19}$$

and E_Δ is the energy stored by the pier in a cycle with maximum ductility equal to μ_Δ:

$$E_d = \frac{\chi_y L}{3} \mu_d M_y \left[1 + \alpha(\mu - 1)\right] \tag{2.20}$$

By substituting Eqs. (2.10), (2.19) and (2.20) into Eq. (2.18), and by making M_{max} and χ_{max} equal to M_y $[1+\alpha\cdot(\mu-1)]$ and $\mu\cdot\chi_y$, respectively, the following expression for the equivalent damping ratio of the member is obtained:

$$\xi_{eq} = 3\eta \frac{\mu}{\mu_\Delta} \cdot \frac{L_p}{L} \tag{2.21}$$

For the evaluation of the plastic hinge length, expressions taken from the literature, such as the one proposed by Priestley and Park [1987], were not used, since from the comparison with the experimental results used as reference in this research [Pinto *et al.* 1995, 1996], it was observed that they generally overestimate the plastic hinge length. All these expressions are empirical and were derived from experimental tests conducted on reinforced concrete specimens made by

concrete and steel rebars with specific mechanical characteristics. According to Manfredi and Pecce [1998], the key parameter that controls the plastic hinge length is the ratio between the ultimate and the yield strength of the reinforcing steel: the higher is this ratio, the longer is the plastic hinge. The formula proposed by Priestley and Park [1987], for example, is derived based on tests conducted on concrete columns reinforced with steel rebars characterized by over strength factors ranging between 1.35 and 1.5. Since the ratio of ultimate to yield strength of the Tempcore steel is approximately equal to 1.19, the formula suggested by Priestley and Park [1987] cannot be applied directly to estimate the length of the plastic hinges expected in modern European bridge piers in which Tempcore steel is used as reinforcement. Furthermore, the expressions presented in the literature do not relate the plastic hinge length with the ductility level of the critical section, contradicting experimental evidence. For all these reasons, curves similar to those shown in Figure 2.4 derived from experimental tests [Pinto *et al.* 1995, 1996] should be used.

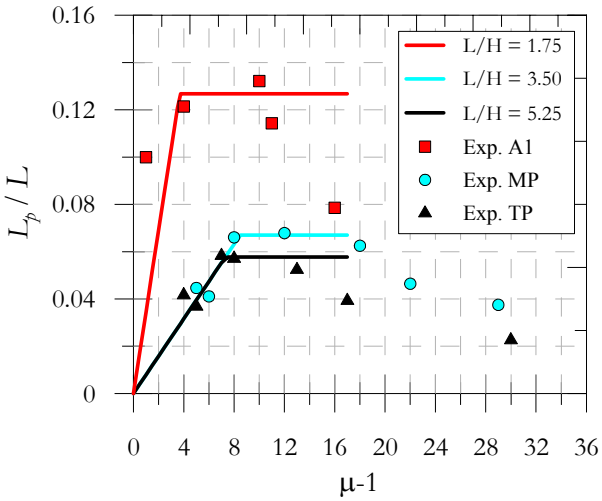

Figure 2.4 Values of the ratio between the plastic hinge length and the pier height as a function of the ductility level of the critical section of the pier and the pier aspect ratio. The proposed piecewise curves are based on the experimental results relative to the A1 pier tested in Pinto et al. [1995] and to the medium and tall pier (MP, TP) of the B213C bridge tested in Pinto et al. [1996]

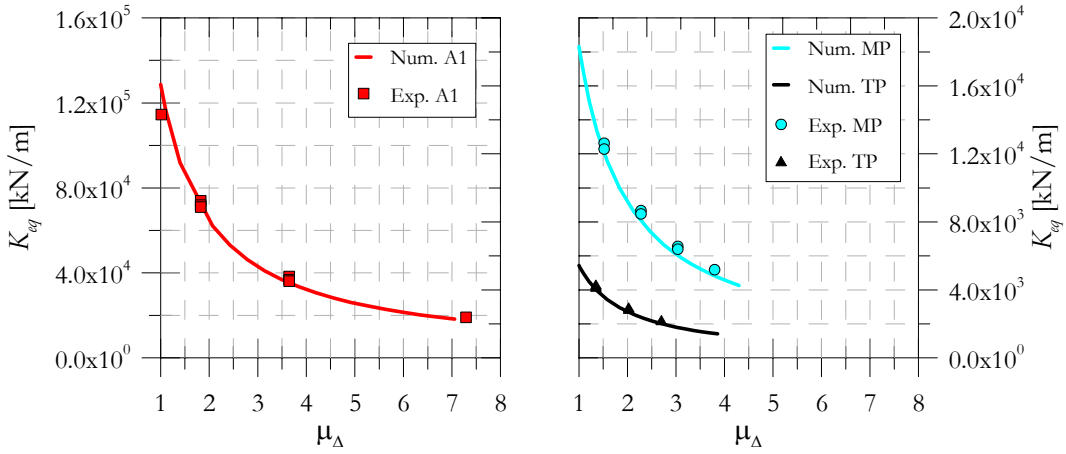

Figure 2.5 Equivalent stiffness in terms of pier ductility: Comparison between the values obtained numerically through the application of the proposed procedure and those obtained experimentally for the A1 pier tested in Pinto et al. [1995] and for the medium and tall pier (MP, TP) of the B213C bridge tested in Pinto et al. [1996]

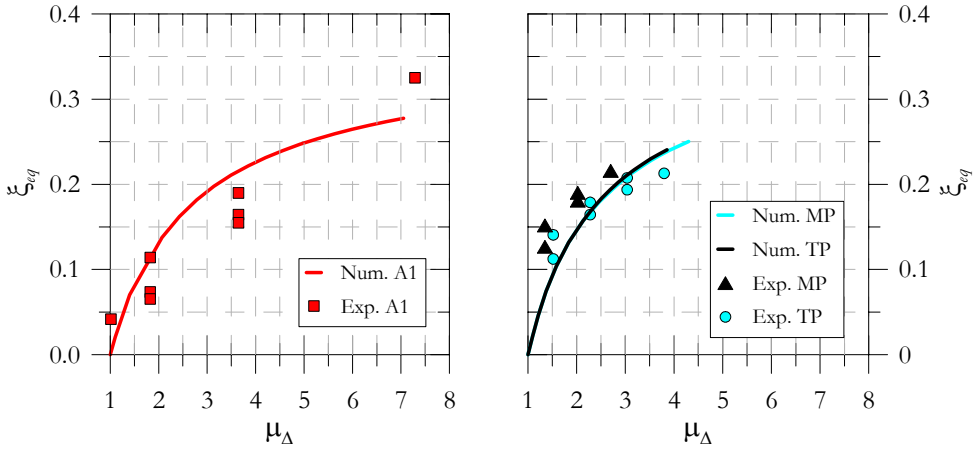

Figure 2.6 Equivalent damping in terms of pier ductility: Comparison between the values obtained numerically through the application of the proposed procedure and those obtained experimentally for the A1 pier tested in Pinto et al. [1995] and for the medium and tall pier (MP, TP) of the B213C bridge tested in Pinto et al. [1996]

As an example, the proposed procedure is applied to derive the equivalent stiffness and damping ratio of the A1 pier tested in Pinto *et al.* [1995] and of the medium and tall (MP, TP) piers of the B231C bridge tested in Pinto *et al.* [1996] (see Figure 2.5 and Figure 2.6). These three piers, constructed using Tempcore steel rebars and C25 concrete (f'_{cm} = 33 MPa), have an aspect ratio H/B of the section equal to 2.0, with H and B equal to 1.6 m and 0.8 m respectively, and a normalised axial force ν_k equal to 0.10. In Table 2.2 are listed the remaining characteristics of these three piers, showing the values of the parameters used to derive the equivalent properties; the length of the plastic hinge was derived from the curves shown in Figure 2.4.

Table 2.2 Parameters used to derive the equivalent stiffness, K_{eq}, and damping ratio, ξ_{eq}, of the A1 pier tested in Pinto et al. [1995]

	A1 pier	MP pier	TP pier
L [m]	2.8	5.6	8.4
ρ_L	0.009	0.012	0.012
λ_c	1.24	1.22	1.22
ρ_w	0.0033	0.0033	0.0033
χ_y [mrad]	3.84	3.81	3.81
M_y [kN·m]	3558	4300	4300
α	0	0	0
μ_u	18	18	18
Δ_y [m]	0.0100	0.0398	0.0896
L_{p0} [m][1]	0.40	0.39	0.49
K_y [MN/m]	127	19.3	5.71
$\mu_{\Delta u}$ [2]	7.1	4.3	3.9

(1) L_{p0} is the plastic hinge length at the plateau of the bilinear curves shown in Fig. 2.4
(2) $\mu_{\Delta u}$ is given by Eq. (2.14) when $\mu = \mu_u$

3. ULTIMATE DEFORMATION AND SHEAR CAPACITY OF CONCRETE PIERS

An important element to achieve and complete the displacement based assessment and design of a reinforced concrete bridge is to have information on the deformation capacity of the piers and on the type of mechanism governing their failure. When performing the design of a bridge, the piers are detailed such that the flexural capacity of the section at the base is achieved while ensuring a sufficient level of shear strength in accordance with the rules of capacity design; the performance of the bridge is then satisfied by detailing the section to provide the required level of displacement capacity of the pier. For assessment, on the other hand, it is necessary to determine first the type of mechanism governing failure, *i.e.*, to establish the relative lateral strengths in shear and in flexure; for members failing in shear, no additional member deformation will be available beyond failure, while for members failing in flexure, the available deformation after yielding is determined as a function of the detailing and geometry of the member and checked against the displacement demand.

Equally important to establishing strength and deformation capacities, is the determination of the deformability or stiffness of the pier resulting from the relative contributions of flexural and shear deformations. In the following two sub-sections, indications are given on how to account for all these variables, that complement the information given in Section 1 and Section 2, necessary to complete the performance based design and assessment of a bridge.

3.1 ULTIMATE DEFORMATION

The displacement capacity of a bridge pier may be evaluated by means of several methodologies that vary in complexity and computational effort, ranging, for example, from the plastic hinge method to Finite Element Model (FEM) analysis.

FEM analysis is used, in general, when detailed and accurate information on the deformability of an element is needed at the expense of high computational cost, such as when performing assessment of very important structures or parts of a structure, or when other more simple approaches do not provide satisfactory results, such as for the case of short piers subjected to the combination of axial, shear and flexural loads. For this case, FEM programs such as ADAPTIC (Izzudin and Elnashai, 1989) and Response 2000 [Bentz, 2000] maybe a viable option. For all other cases, such as when performing design or assessment using simplified methods, the use of FEM analysis is not feasible and the plastic hinge method is proposed instead as a more computationally efficient and sufficiently accurate option for assessment and design.

The plastic hinge method, in general, gives good estimates of load-deformation response for members where the relative contribution of shear with respect to flexural deformation is not important, *i.e.*, for members with shear span-to-depth ratios larger than 2.0~2.5. For members with low shear span-to-depth ratios where the contribution of shear deformation is relevant, the plastic hinge approach may still be used, following the approach exposed later in this section.

The expressions based on the plastic hinge method used to determine the load-deformation curves of rectangular reinforced concrete hollow piers as derived from experimental tests have already been presented in Section 2. In this section, emphasis will be given to the determination

of the plastic hinge length and to the design or assessment of a bridge pier against target performance when flexural failure is the controlling mechanism.

According to the plastic hinge method, the displacement at the top of a cantilever pier of length L is computed as the sum of the contribution of the deformations from a plastic and an elastic region, defined as a function of the distribution of curvatures along the member. The curvatures along the plastic region span over a length L_p and are considered constant and equal to the curvature at the critical section of the member, while the curvatures along the elastic region decrease linearly to zero from the curvature at yield. The displacement Δ at the top of the pier is then computed from the first moment of inertia of the curvature distribution about the top of the pier:

$$\Delta = \frac{\chi_y \cdot L^2}{3} + \left(\chi_{\max} - \chi_y\right) \cdot L_p \cdot \left(L - \frac{L_p}{2}\right) \qquad (3.1)$$

where $\chi_{\max}$ and χ_y are the maximum and the yield curvatures at the critical section of the pier, respectively, and L_p is the plastic hinge length. Eq. (3.1) considers that the behaviour of the pier is elasto-plastic (post-yield stiffness ratio α of the section equal to zero), which is a valid approximation for bridge piers reinforced with Tempcore steel and detailed to undergo plastic deformations (*i.e.*, λ_c>1). The length of the plastic hinge may be computed from the results of experimental tests by solving Eq. (3.1), such that for the maximum curvature measured at the base of the pier at different ductility levels, the corresponding maximum displacement measured at the top of the pier is obtained; the yield curvature is assessed from the experimental moment-curvature diagram of the section. Following this procedure and using the experimental results from Pinto *et al.* [1995, 1996], the values of L_p, presented graphically in Section 2 for the tall, medium and short piers, were obtained as a function of the curvature ductility μ of the critical section, as expressed by the following expression:

$$\begin{cases} \dfrac{L_p}{L} = c_L \cdot \dfrac{\mu - 1}{\mu_L - 1} & \text{with} \quad 1 \le \mu \le \mu_L \\ \dfrac{L_p}{L} = c_L & \text{with} \quad \mu \ge \mu_L \end{cases} \qquad (3.2)$$

where c_L and μ_L are two parameters that depend on the shear span-to-depth ratio a/d, and are equal, for the medium and tall piers (a/d equal to 3.5 and 5.3), to 0.0624 and 9, and for the short pier (a/d equal to 1.8), to 0.127 and 5, respectively. Since these results were derived from a very limited number of tests, it would be desirable that a larger set of experimental data is used to increase the reliability of the proposed curves.

An important feature of the procedure exposed above to calculate the length of the plastic hinge is that it allows to determine in a simplified manner the flexibility of a short pier, accounting in an empirical way for the contribution of shear deformations that otherwise would need to be obtained from more refined and computationally expensive analytical methods (See the first paragraph of this Section).

The displacement capacity Δ_u of a cantilever pier is computed from Eq. (3.1), by substituting Δ with Δ_u and $\chi_{\max}$ with $\chi_u = \chi_y \cdot \mu_u$, so that for a given a/d ratio (*i.e.*, the parameters c_L and μ_L are known) the displacement capacity Δ_u remains a sole function of the ultimate curvature ductility μ_u that the section can develop at the base of the pier.

The ultimate curvature ductility μ_u is obtained from the charts presented in Figure 2.2 of Section 2, derived for reinforced concrete rectangular hollow piers as a function of the H/B aspect ratio,

the percentage ρ_L of longitudinal steel reinforcement, the normalized axial force ν_k, the confinement level λ_c of the section (Mander's parameter, as defined in Annex E of EN1998-2 [CEN, 2005]), and the mean values f_{cm} and f_{ym} corresponding to the concrete compressive and steel yield strengths. The ultimate curvature ductility μ_u was computed numerically using a fibre model and corresponds to the state when either the first concrete fibre reaches its ultimate compressive strain $\varepsilon_{cu,c}$ as determined from Eq. (2.3) of Section 2, or when the longitudinal reinforcement reaches its ultimate strain in compression or tension, or when the strength of the section decreases to 80% of its maximum value.

In Figure 3.1 is shown the range of variation of μ_u for different section aspect ratios and amounts of longitudinal reinforcement for all the considered values of ν_k and λ_c, with f_{cm} and f_{ym} equal to 33 MPa and 575 MPa, respectively. From the chart it can be observed that the maximum value of μ_u decreases as the aspect ratio or the amount of longitudinal reinforcement increases, while the minimum value of μ_u remains practically constant. This chart is important as it gives an indication of the upper bound of μ_u, which may be useful when performing a rapid screening of the deformation capacity of a bridge pier.

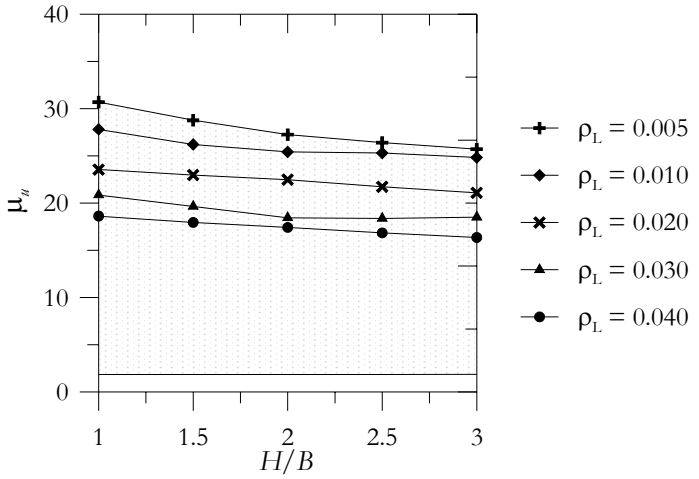

Figure 3.1 Range of variation for the ultimate curvature exhibited by hollow reinforced concrete pier sections with different values of aspect ratio, *H/B*, and longitudinal reinforcement ratio, ρ_L

The information contained in the charts of Figure 2.2 of Section 2 may be rearranged and expressed in such a way so as to give direct information on the displacement capacity of a pier of a given aspect ratio H/B and normalized axial force ν_k. This is done by plotting the variation of the ultimate curvature ductility μ_u as a function of λ_c for different percentages of ρ_L, together with the field of variation of μ_u as a function of the target performance of the pier, as shown in Figure 3.2 and Figure 3.3 for a pier section with H/B equal to 2 and ν_k equal to 0.1. The target performance may be defined, for example, in terms of a maximum displacement ductility μ_Δ, of a maximum drift δ, or of a maximum displacement Δ the pier.

If the maximum displacement ductility of the pier is used as target performance, the variation of μ_u as a function of μ_Δ may be expressed by rearranging Eq. (3.1) and by substituting Δ with $\Delta_y \cdot \mu_\Delta$, and $\Delta_y = \chi_y \cdot L^3/3$, so that the following expression is obtained:

$$\mu_u = 1 + \frac{1}{3 \cdot \frac{L_p}{L} \cdot \left(1 - 0.5 \cdot \frac{L_p}{L}\right)} \left[\mu_\Delta - 1\right] \qquad (3.3)$$

where L_p/L is given by Eq. (3.2) after substituting μ with μ_u. Note that for $\mu_u < \mu_L$, L_p/L is a function of μ_u, so that Eq. (3.3) needs to be solved iteratively for μ_u. The plot of Eq. (3.3) for μ_Δ equal to 2, 3 and 4 is given in the chart of Figure 3.2 for the medium and tall piers. Note that for a given value of μ_Δ, μ_u is constant and independent of λ_c. The chart suggests that an increase of the section confinement (*i.e.*, of λ_c) with the purpose of achieving a larger displacement ductility capacity of the pier is most advantageous at large values of ρ_L.

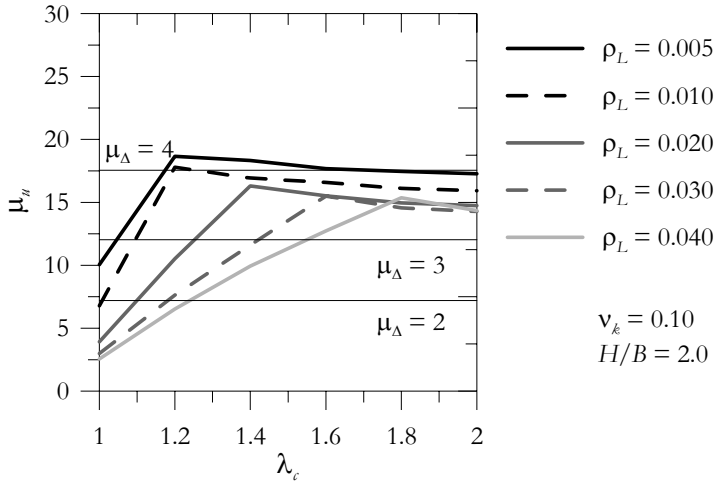

Figure 3.2 Proposed chart for the design of hollow rectangular piers with ν_k =0.10 and H/B =2.0, using displacement ductility, ν_Δ, as performance parameter

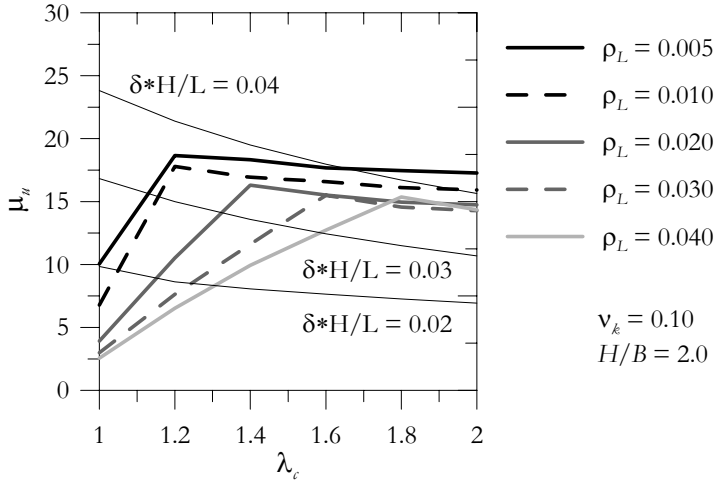

Figure 3.3 Proposed chart for the design of hollow rectangular piers with ν_k =0.10 and H/B =2.0 using drift, δ, as performance parameter

If the maximum drift δ of the pier is used as target performance, the variation of μ_u with respect to δ is obtained by expressing μ_Δ as:

$$\mu_\Delta = \frac{\delta \cdot L}{\Delta_y} \tag{3.4}$$

so that by substituting Eqs. (2.13) and (2.8) from Section 2 into Eq. (3.4), which is then substituted into Eq. (3.3), the following equation is obtained:

$$\mu_u = 1 + \frac{1}{3 \cdot \frac{L_p}{L} \cdot \left(1 - 0.5 \cdot \frac{L_p}{L}\right)} \left[\frac{3}{0.00552\sqrt{\lambda_c}} \frac{\delta \cdot H}{L} - 1 \right] \qquad (3.5)$$

In the same way as for Eq. (3.3), Eq. (3.5) needs to be solved iteratively for μ_u when μ_u is less than μ_L. The plot of Eq. (3.5) as a function of λ_c for the non-dimensional values $\delta H/L$ corresponding to 0.02, 0.03 and 0.04 is given in Figure 3.3 for the medium and tall piers.

The use of these charts is illustrated in the following example for a section with H/B=2 and ν_k =0.1. For assessment, suppose the section is detailed with ρ_L equal to 0.04 and λ_c equal to 1.3, then the chart indicates that the maximum displacement ductility and maximum drift that the pier can develop is equal to 2.2 and $0.02 \cdot L/H$, respectively. Likewise, for design, suppose that the target displacement ductility is equal to 3.3 or that the target drift is equal to $0.03 \cdot L/H$, with the constraint of developing a minimum flexural strength corresponding to ρ_L equal to 0.03, then the chart indicates that the section should be confined with a detailing corresponding to λ_c equal to 1.48. Note that the two target performances are not equivalent (*i.e.*, they do no lead to the same pier displacement), however, they were chosen such that for the example the same value of λ_c would be obtained from the two charts.

For the case where the maximum displacement Δ is used as target performance, it is sufficient to substitute into Eq. (3.6) and in Figure 3.3 the term $\delta H/L$ by $\Delta \cdot H/L^2$.

In practice, for each target performance parameter, being μ_Δ or $\delta H/L$, and for each a/d ratio of the pier (different parameters ω_L and μ_L), 20 charts are needed to consider all the combinations of H/B (five values, varying from 1 to 3 at a step of 0.5) and ν_k (four values, varying from 0.1 to 0.4 at a step 0.1) considered in the analysis. It is foreseeable that all piers with a/d in excess of 2~2.5 may be grouped under the same chart, with ω_L and μ_L values similar to those derived for the medium and tall piers. In the charts where maximum displacement ductility is the target performance, μ_Δ may be varied from 1 to 5 at a step of 0.5, while for the charts where drift or displacement is the target performance, $\delta H/L$ may be varied from 0.01 to 0.045 at a step of 0.005. The dependence of these charts on the concrete compressive and steel yield strengths, as well as on the width of the pier section, should not be relevant.

3.2 SHEAR CAPACITY

This section presents a brief review on the shear capacity of reinforced concrete bridge piers. The presentation is centred on the discussion of the methods available in literature to compute the capacity of tall or slender piers, and short piers.

For tall piers, where flexural deformations prevail with respect to shear deformations, the deformations of the pier are modelled through plane section behaviour, and the so-called truss models are proposed to assess the shear capacity of the member. Several truss models are reviewed, and the way that the concrete and the transverse steel reinforcement contributions to shear strength are taken into account is discussed, in particular, with reference to the effects of axial compression, displacement ductility, and shear span-to-depth ratio of the pier. A simplified method based on the Modified Compression Field Theory (MCFT) is also presented, that takes into account the interaction of flexural, shear and axial forces on the section. For the case of short piers, where the contribution of shear deformations to the total displacement of the pier is important, the strut and tie method is presented as an alternative simplified technique to compute shear strength.

The expressions presented to compute shear strength, in large part derived for rectangular and circular solid sections, are assessed against experimental results obtained from PsD earthquake tests performed on a bridge structure with reinforced concrete hollow piers.

3.2.1 Truss Models

When a reinforced concrete member is subjected to transverse loads, its shear failure may occur due to either diagonal tension failure or diagonal compression failure. Diagonal tension failure results from disruption of the load carrying mechanisms of the member (*e.g.*, contribution of the transverse reinforcement and of the concrete in compression, aggregate interlock, dowel effect) following the formation of inclined cracks with respect to the member axis. Failure in compression results from crushing of the concrete strut that forms in the web of the member and may occur before or after the formation of inclined cracks, when either the column axial force or the transverse reinforcement ratio, or both, are relatively high, or alternatively, if the aspect ratio[1] is relatively low.

Current design procedures for reinforced concrete members in shear stem from the original truss model proposed by Ritter [1899] and Mörsch [1909] that state that for elements with an aspect ratio greater than 2 with axial load near or below the balanced point, diagonal tension failure is the controlling mechanism. In this model it is assumed that a cracked reinforced concrete beam acts like a truss with parallel longitudinal chords and a web composed of steel ties and diagonal concrete struts inclined 45° with respect to the longitudinal axis (Figure 3.4); the tensile stresses in the diagonally cracked concrete are neglected. According to this model, when transverse loads act on a reinforced concrete member, the diagonal compressive concrete stresses push apart the loaded faces, while the tensile stresses in the stirrups pull them together. I view of these considerations the shear resistance is computed as:

$$V = \frac{A_v \cdot d_v \cdot f_{yy}}{s} \tag{3.6}$$

where A_v is the area of shear reinforcement within a distance equal to the stirrup spacing s, d_v is the effective shear depth taken as the flexural lever arm of the member and f_{yy} is the yield stress of the shear reinforcement.

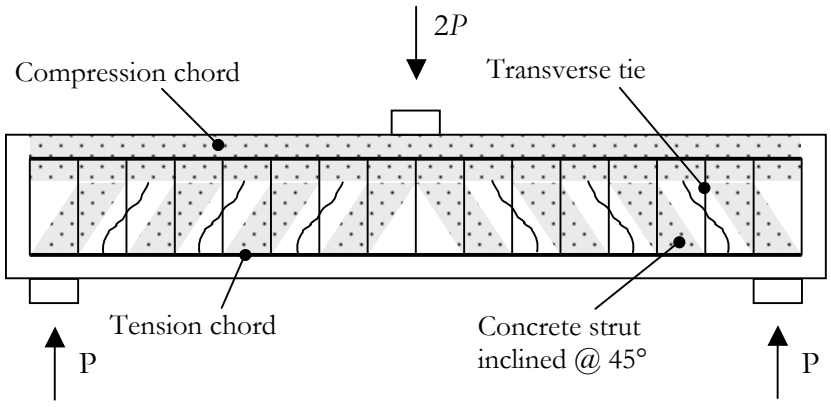

Figure 3.4 Ritter-Morsch model

[1] The aspect ratio of an element is defined as the ratio between the shear span and the width of the element cross section.

Experimental tests have revealed that the results given by the model proposed by Ritter and Mörsch are generally quite conservative. In fact, the model neglects important sources of shear resistance such as aggregate interlock, dowel action of the longitudinal steel and shear carried across the uncracked concrete, as well as the effects of axial force on shear resistance.

For this reason, most construction standards and norms (*e.g.*, ACI 318–2002, CSA - Canadian Standard Association 1994) have accepted to add an empirical correction term to the original truss equations. This term, known as the "concrete contribution", and generally denoted as V_c, is meant to represent those sources of shear resistance that the basic truss model does not take into account. With this assumption, the shear resistance can be expressed as:

$$V = V_s + V_c \tag{3.7}$$

where V_s and V_c represent the transverse reinforcement and concrete contributions to shear resistance, respectively. The transverse reinforcement contribution is given by Eq. (3.6), while the concrete contribution is taken as the shear force corresponding to the initiation of diagonal cracking, as derived from experimental tests and expressed, for example, from the following empirical expressions as found in the ACI and CSA construction codes:

$$\text{ACI 318 - 2002} \quad V_c = 0.166 \cdot \left(1 + \frac{P}{13.8 \cdot A_g}\right) \cdot \sqrt{f_c'} \cdot b \cdot d_v \quad \text{(MPa)} \tag{3.8}$$

$$\text{CSA 1994} \quad V_c = 0.20 \cdot \sqrt{f_c'} \cdot b \cdot d_v \quad \text{(MPa)} \tag{3.9}$$

where f'_c is the compressive strength of concrete, b is the width of the member, d_v is the effective depth of the member, A_g is the gross area of the member section, and P is the axial load (positive if compressive).

When comparing Eqs. (3.8) and (3.9), it is possible to observe that only the first equation takes into account the effect of axial force on shear resistance: axial compressive loads increase the shear load at which flexural and inclined cracking initiate. The dependency of V_c on the axial load may be thought as a way to account for the effects of axial loads on the shear mechanisms neglected in the Ritter-Mörsch truss model, *i.e.*, axial compression forces generate a larger compression zone characterized by a greater shear strength; on the contrary, axial tensile forces reduce the depth of the compression zone and leading to premature yielding of the longitudinal reinforcement, which in turn rapidly destroys the aggregate interlock mechanism. It is worth noting that some codes (*e.g.*, ACI 318-89) consider the beneficial effect of axial loads on shear resistance only for the case of axial forces coming from external sources, such as gravity loads, while for axial forces generated from self-equilibrated systems, no beneficial effects are considered.

Acknowledging the conservative results given by the Ritter-Mörsch truss model, the European Norm EN 1992-1-1 [CEN, 2004] does not use the corrective term V_c, instead adopts a method known as the "variable – angle truss method"[2], which is based on a truss model in which the concrete struts form with the member axis an angle θ that can vary up to a value of 45°. The method recognises that due to shear mechanisms different from those considered by the Ritter–Mörsch truss model, the compressive stresses in the member web may have an inclination lower than 45°. According to this model the shear resistance of a member may be reached either for yielding of the stirrups:

---

[2] A combination of the variable-angle truss and concrete contribution methods, known in literature as the modified truss model approach, has been proposed by CEB [1978] and Ramirez and Breen [1991].

$$V = \frac{A_v}{s} \cdot d_v \cdot f_{vy} \cdot \cot\theta \tag{3.10}$$

or for crushing of the concrete web struts:

$$V = b \cdot d_v \cdot \nu \cdot f_c' / \left(\cot\theta + \tan\theta\right) \tag{3.11}$$

where ν is the strength reduction factor for concrete cracked in shear and is computed as a function of the compressive stress f'_c derived from cylinder tests:

$$\nu = 0.6 \cdot \left(1 - \frac{f_c'}{250}\right) \quad (f_c \text{ in MPa}) \tag{3.12}$$

Eq. (3.12) accounts for the lower compression resistance of the concrete forming the struts with respect to that derived from standard cylinder tests. This reduction in resistance is due to the high tensile strains that exist in the direction normal to the struts and to the mechanical disturbance caused by the stirrups crossing the struts.

The angle θ is computed such that shear resistance is attained when yielding of the shear reinforcement and crushing of the web concrete struts are reached simultaneously, leading to the following equation:

$$\cot\theta = \sqrt{\frac{1-\omega_v}{\omega_v}} \tag{3.13}$$

expressed as a function of the mechanical percentage of web reinforcement ω_v:

$$\omega_v = \frac{A_v \cdot f_{vy}}{s \cdot b \cdot \nu \cdot f_c'} \tag{3.14}$$

The EN 1992-1-1 Norm [CEN, 2004] also allows to choose a value of $\cot\theta$ between 1 and 2.5 ("recommended" values) and to use as shear resistance of a member the lowest value resulting from Eqs. (3.10) and (3.11). For members subjected to axial compressive forces, the same code suggests to multiply the value given by Eq. (3.11) by a factor α_c ranging between 0 and 1.25, depending on the mean compressive stress σ_p acting on the section of the member. EN 1992-1-1 [CEN, 2004] does not consider any distinction between the source of the loads inducing the compressive stresses, which may be either external (*i.e.*, gravity loads) or internal due to prestressing or postensioning. It should be noted that EN 1992-1-1 [CEN, 2004] does not give any indication on how to account for the effects on shear resistance associated to loads inducing tensile stresses on the section.

Both of the approaches presented in the previous paragraphs (*e.g.*, concrete contribution and the variable angle truss method) do not take into account the reduction in shear resistance as the deformation of the section increases or after several cycles of load reversal. In view of the difficulty of modelling the deterioration of mechanisms such as tension stiffening, aggregate interlock and dowel action with the increase of member deformations, a number of codes reduce or even neglect the concrete contribution term. For example, in the case of bridges subjected to seismic actions, EN1998-2 [CEN, 2005] suggests to assume a value of θ equal to 45° when designing plastic hinge regions for shear, *i.e.*, the Ritter-Mörsch truss model is adopted with no concrete contribution. For bridge piers with shear span-to-depth ratios less than 2, EN1998-2 [CEN, 2005] calculates the shear strength based on the verification of the pier against diagonal tension and sliding failure in accordance with EN1998-1 [CEN, 2004].

In other codes, the concrete contribution reduction depends on the value of the compressive stress: if it is less than a small fraction of f'_c, it is set equal to zero, otherwise it is taken as a fraction of its value derived from static tests, as given for example by Eqs. (3.8) and (3.9). Unfortunately, experiments have shown that the estimate of shear strength resulting from these equations is over-conservative at low values of displacement ductility demand and under-conservative at high values of displacement ductility.

The dependence of shear strength on deformation demand has been acknowledged as early as 1975 in a comprehensive study of reinforced concrete columns subjected to large displacement reversals [Wight and Sozen, 1975]. In 1983, the Applied Technology Council [ATC, 1983] published guidelines for seismic retrofit of bridges in which a conceptual model was proposed to model the relationship between shear demand and supply at different ductility levels (Figure 3.5), which has inspired some of the contemporary approaches to model the concrete contribution term in the guidelines of design codes.

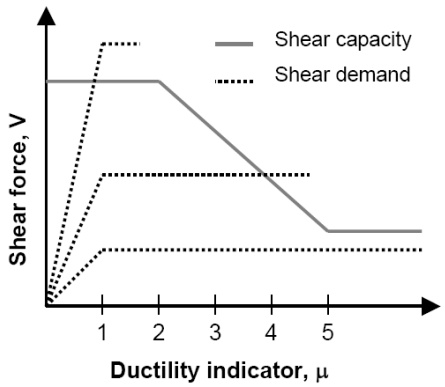

Figure 3.5 Applied Technology Council Model for shear strength degradation

Most of the proposed models consider a constant initial value for V_c up to a displacement ductility of 1 [Wong *et al.*, 1993; Lehman *et al.*, 1996] or 2 [Ang *et al.*, 1989; Priestley *et al.*, 1994], decaying linearly to a residual value at large displacement ductilities. For example, Lehman *et al.* [1996] set the residual value of V_c equal to zero for displacement ductilities larger than 4.

In the experimental studies carried out by Ang *et al.* [1989], Aschheim and Moehle [1992] and Wong *et al.* [1993] it has been observed that the concrete contribution is enhanced by an increase in the amount of shear reinforcement. This behaviour is represented by the models proposed by Ang *et al.* [1989], where the concrete residual shear strength is proportional to the amount of transverse reinforcement, and by the model of Aschheim and Moehle [1992], where the overall concrete shear contribution increases with the amount of transverse reinforcement. In the experimental studies by Ang *et al.* [1989] and Wong *et al.* [1993] it was also observed that when the flexural ductility increases to values above two, the inclination of the diagonal compression struts of the truss mechanism with respect to the longitudinal axis decreases ($\theta < 45°$), thus increasing the shear carried by the transverse reinforcement and hence that of the overall truss.

Two models, Priestley *et al.* [1994] and Sezen and Moehle [2004], that take into account the effects of axial load and ductility demand on shear strength, are hereafter discussed.

According to Priestley *et al.* [1994], the shear strength of columns subjected to cyclic lateral loads results from the summation of three contributions: concrete, V_c; a truss mechanism, V_s; and an arch mechanism, V_p:

$$V = V_c + V_s + V_p \tag{3.15}$$

The concrete component is given by:

$$V_c = k \cdot \sqrt{f_c'} \cdot \left(0.8 \cdot A_g\right) \qquad \text{(MPa)} \tag{3.16}$$

in which the parameter k, defined in Figure 3.6 for plastic end regions, depends on the member displacement ductility demand; for regions of columns outside the plastic end region, the concrete component is computed with the value of k corresponding to a ductility demand of one. The model assumes hat crack opening leads only to degradation of the load-carrying capacity of concrete, with no associated degradation of the reinforcement.

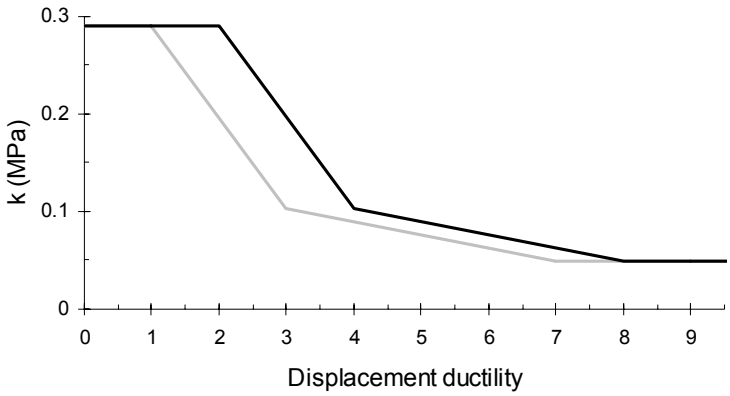

Figure 3.6 Relationship between ductility and strength of concrete shear-resisting mechanisms (adapted from Priestley et al. [1994])

The contribution of transverse reinforcement to shear strength is based on a truss mechanism using an angle θ equal to 30°. For rectangular columns this contribution is given by:

$$V_s = \sqrt{3} \cdot \frac{A_v \cdot f_{ry} \cdot D'}{s} \tag{3.17}$$

and for circular columns by:

$$V_s = \frac{\pi}{2} \cdot \sqrt{3} \cdot \frac{A_h \cdot f_{ry} \cdot D'}{s} \tag{3.18}$$

where A_h is the area of one hoop leg; s is the spacing of the layers of stirrups or hoops along the member axis; A_v is the total area of transverse reinforcement in a layer along the direction of the shear force; D' is the core dimension from centre to centre of the stirrup or peripheral hoop.

The shear strength enhancement resulting from axial compression is considered as an independent component of shear strength, resulting from the contribution of the diagonal compression strut shown in Figure 3.7:

$$V_p = P \cdot \tan\alpha \tag{3.19}$$

For a cantilever column, α is the angle formed between the column axis and the strut extending from the point of load application to the centre of the flexural compression zone at the column plastic hinge critical section. For a column in reverse or double bending, α is the angle between

the column axis and the line joining the centres of flexural compression at the top and bottom of the column.

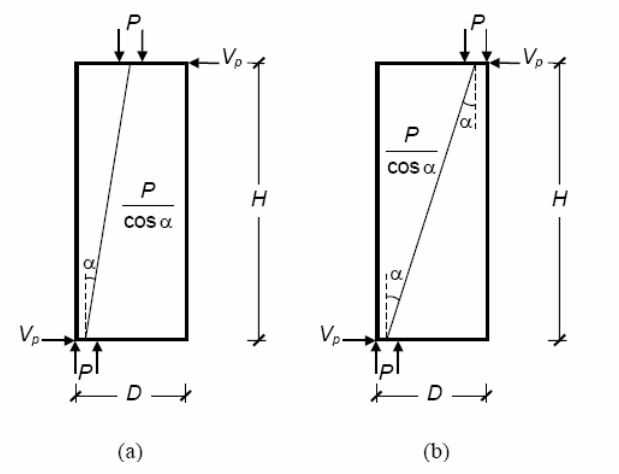

Figure 3.7 Contribution of axial force to column shear strength for (a) simple bending and (b) reversal bending (adapted from Priestley et al. [1994])

More recently, Sezen and Moehle [2004] have proposed a shear strength model for lightly reinforced concrete columns similar to the one introduced by Priestley *et al.* [1994], where the k factor is applied to both the concrete and truss contributions. Sezen and Moehle [2004] recognize that the damage of concrete leads to a loss of anchorage of the transverse reinforcement and to a reduction in the bond capacity of the longitudinal and transverse reinforcement, thus reducing the strength of the truss mechanisms. Based on these assumptions and considering a truss model with θ equal to 45°, the shear strength is expressed by the following equation:

$$V = V_s + V_c$$
$$= k \cdot \frac{A_v \cdot f_{yy} \cdot d}{s} + k \cdot \frac{0.8 \cdot A_g \cdot 0.5 \cdot \sqrt{f_c'}}{a/d} \cdot \sqrt{1 + \frac{P}{0.5 \cdot \sqrt{f_c'} \cdot A_g}} \quad \text{(MPa)} \quad (3.20)$$

for shear span-to-depth ratios, a/d, comprised between 2 and 4. The k factor is defined equal to 1.0 for displacement ductilities less than 2 and equal to 0.7 for displacement ductilities exceeding 6, varying linearly for intermediate displacement ductilities.

3.2.2 Modified Compression Field Theory (MCFT)

The compression field theory (CFT) is a procedure for the shear design of reinforced concrete members that determines the inclination angle θ of the compressive struts in a truss model following the principles of the tension field theory developed by Wagner [1929]. Equilibrium conditions, compatibility conditions and stress-strain relationships for both the reinforcement and the diagonally cracked concrete are used in the CFT to predict the load-deformation response of a member subjected to shear. The CFT methods that account for the tensile strength of concrete are known as Modified Compression Field Theory (MCFT) methods [Vecchio and Collins, 1986], [Bhide and Collins, 1989], [Collins and Mitchell, 1991].

Collins and Mitchell [1991] have proposed a simplified hand-based design method derived from MCFT, which has been adopted by a number of codes, such as the Ontario Highway Bridge Design Code [1991], the Norwegian Code [1992], the Canadian Standards Association Concrete Design Code [2004] and the AASHTO LRFD [2004] specifications.

Although Vecchio [1999] and Palermo and Vecchio [2003] have shown that the MCFT can be used to model the effects of reversed cyclic loads on reinforced concrete members, the AASHTO LRFD [2004] specifications use the MCFT design approach only for static actions; for seismic actions, AASHTO LRFD [2004] adopts a model similar to that proposed by Priestley [1994].

Hereafter, the simplified MCFT procedure adopted by CSA [2004] to compute the amount of transverse reinforcement necessary to design a section subjected to bending, axial and shear forces, M_u, N_u (negative if compressive) and V_u, is briefly presented. The methodology is applicable if the shear force demand satisfies the following condition:

$$\frac{V_u}{\phi} < 0.25 \cdot f_c' \cdot b \cdot d_v \tag{3.21}$$

where ϕ is equal to 0.9.

The first step of the design procedure consists in the calculation of the longitudinal strain ε_x at mid-depth of the section (see Figure 3.8, assuming $\cot\theta = 2$ and $\varepsilon_x = \varepsilon_t / 2$):

$$\varepsilon_x = \frac{\left(M_u/d_v\right) + 0.5 \cdot N_u + V_u}{2 \cdot \left(E_s \cdot A_s + E_c \cdot A_{ct}\right)} \geq -0.2 \cdot 10^{-3} \tag{3.22}$$

where A_s and A_{ct} are the areas of longitudinal reinforcement and concrete on the flexural tension side of the beam, and E_s and E_c are the steel and concrete Young's modulus, respectively; the term A_{ct} is equal to zero for $\varepsilon_x \geq 0$. The concrete contribution is calculated as:

$$V_c = 0.0830 \cdot \beta \cdot \sqrt{f_c'} \cdot b \cdot d_v \quad \text{(MPa)} \tag{3.23}$$

where:

$$\beta = \frac{4.8}{1 + 1500 \cdot \varepsilon_x} \cdot \frac{129.54}{99.06 + s_{xe}} \quad \text{(cm)} \tag{3.24}$$

and s_{xe} is the equivalent crack spacing equal to 30.48 cm. (*i.e.*, 12 inches).

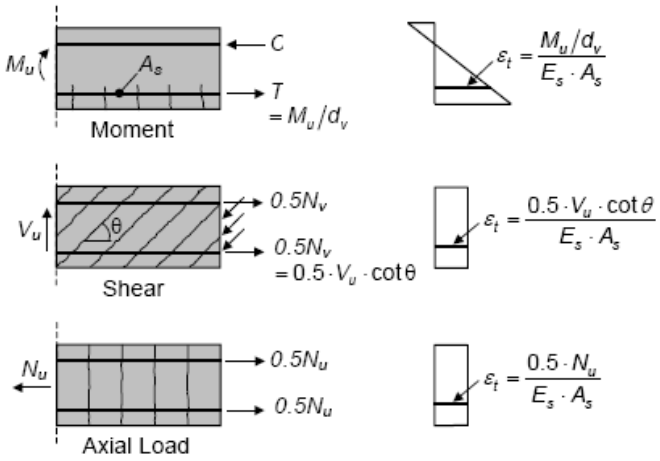

Figure 3.8 Determination of strain ε_x for a non-prestressed beam (adapted from ASCE-ACI Committee 445 on shear and torsion [1998])

The portion of shear strength supplied by the shear reinforcement is given by:

$$V_s = \frac{V_u}{\phi} - V_c \tag{3.25}$$

and that the required amount of shear reinforcement is computed as:

$$\frac{A_v}{s} = \frac{V_s}{f_{ry} \cdot d_v \cdot \cot\theta} \tag{3.26}$$

with:

$$\theta = 29 + 7000 \cdot \varepsilon_x \quad \text{(degrees)} \tag{3.27}$$

The amount of shear reinforcement must be larger or equal than the minimum required by the code:

$$A_{v,\min} = 0.0830 \cdot \sqrt{f_c'} \cdot \frac{b \cdot s}{f_{ry}} \quad \text{(MPa)} \tag{3.28}$$

Although not explicitly envisaged by CSA [2004], it is possible to assess the shear strength V_s + V_c of a member designed with transverse reinforcement A_v spaced at a distance s and subjected to bending and axial forces M_u and N_u, by iterating on a predicted value of V_u until convergence on V_u is reached.

When performing assessment, the amount of transverse reinforcement may be lower than the minimum required by the code; in this case s_{xe} is computed from the following expression:

$$s_{xe} = \frac{3.51 \cdot s_x}{1.60 + a_g} \quad \text{(cm)} \tag{3.29}$$

where s_x is the smaller between d_v and the maximum distance between layers of crack control reinforcement; a_g is equal to the maximum aggregate size.

A more accurate prediction of the shear strength of a member may be obtained from the exact formulation of the MCFT, through the use of special purpose software as implemented by Bentz [2000].

3.2.3 Strut-and-tie models

The "strut and tie" model is a methodology that allows to compute the shear strength of members wit low shear span-to-depth ratios based on the equilibrium of forces flowing from the point of load application to the location of load transfer. Strut and tie models are generally applied to the so called disturbed or D-regions of members, where arch action, as opposed to beam action (i.e., plane sections remain plane) is exhibited. D-regions extend about one member depth at both ends from the concentrated loads, reactions, or abrupt changes in the section or direction of the member. The shear span-to-depth ratio for which strut and tie models should be used in favour of the "truss models" to compute the shear strength of members is between 2.0 and 2.5.

Schläich *et al.* (1987) suggest two guidelines in selecting a workable strut-and-tie model:

- The compatibility of deformations may be approximately considered by orienting the struts and ties within 15° of the force systems obtained from a linear elastic analysis of uncracked members and connections.
- The most valid model tends to be one which minimizes the amount of reinforcement, since this corresponds to the minimum strain energy solution.

Marti (1985) recommends three rules when using strut-and-tie models:

- Draw truss models to scale.
- Visualize the force flow using consistent equilibrium considerations.
- Ensure that truss member forces can be developed and transferred at the required locations.

More details about the strut-and-tie approach can be found in the ASCE-ACI Committee 445 on shear and torsion [1998].

3.2.4 Comparison against test results

The use of the proposed expressions to compute the shear strength of a reinforced concrete rectangular hollow bridge pier is given in the following; the results are compared with those obtained from the tests performed on the B213C bridge tested by Pinto et al. [1996]. Only the expressions corresponding to the truss models and the MCFT are considered and compared with the experimental results obtained from the tall and medium piers of the tested bridge.

The dimension of the cross section of the piers is 1.6 x 0.8 m, with a wall thickness of 16 cm. The flanges are each detailed with longitudinal reinforcement corresponding to 14-ϕ14 + 6-ϕ12 mm bars (A_s = 2833 mm², area of longitudinal steel in tension); the webs are detailed with transverse reinforcement corresponding to a total cross section of 4-ϕ5 mm bars (A_v = 78.5 mm²). For evaluation purposes, the compressive strength of concrete f_c and the yield strength of steel f_y are taken as their mean values, equal to 33 MPa and 575 MPa, respectively. The same mean yield strength is considered in the analysis for both the longitudinal and the transverse steel, in spite of the higher yield strength, on the order of 700 MPa, obtained from tests performed on 5 mm diameter specimens of the transverse reinforcement. The normalized axial force ν_k is equal to 0.l.

The shear strength of the piers is computed at the base and at a height of 1.5 m, which differ on the amount of transverse reinforcement (60 mm and 80 mm, respectively), and on the level of bending moment to which they are subjected. No reduction factors on the materials or on the overall capacity of the section are used for calculating the shear strength.

The results from the tests show that the maximum shear capacity of the tall and medium piers was attained at a global ductility of 3.9 and 4.75, respectively; failure of the piers, in both cases, was controlled by flexure.

The results of the comparison between experimental and analytical results are summarised in Table 3.1 and show that the strength computed by all expressions is always higher than that obtained from the tests, thus confirming that failure occurred in flexure. Although the tests do not give any information on the actual shear strength of the member, and thus do not allow inferring on the accuracy of the proposed expressions, important conclusions can be derived by comparing the relative strengths. For example, the most conservative measures of strength are given by EN1998-2 [CEN, 2005] and CSA [2004], while Sezen and Moehle [2004] and in particular, Priestley et al. [1994], give higher estimates of the available shear strength. The higher values of strength given by the last two expressions are due to the higher contribution of

concrete, increased by the effect of the compressive axial force. In addition, the steel contribution in Priestley et al. [1994] is increased by a factor of 1.73, as the inclination θ of the concrete struts is made equal 30º.

Table 3.1 Comparison between the shear strength computed from EN1998-2 [CEN, 2005], Priestley et al. [1994], Sezen and Moehle [2004], and MCFT CSA [2004], and the shear capacity obtained from tests on the B213C bridge tested by Pinto et al. [1996], for the tall and medium piers at different sections and ductility levels.

Type of pier Section description	**Shear strength [kN]**				
	V_{test}*	**EN1998-2**	**Priestley *et. al***	**Sezen and Moehle**	**MCFT CSA**
Tall, L/H = 5.25					
x=1.5 m, s=80 mm μ_Δ=1	540	2013#	2612	1318	1097
x=0.0 m, s=60 mm μ_Δ=1	540	1074	3124	1616	1194
x=0.0 m, s=60 mm, μ_Δ=3.9	540	1074	2578	1386	1194
Medium, L/H = 3.5					
x=1.5 m, s=80 mm μ_Δ=1	800	2013#	2706	1529	**1163**
x=0.0 m, s=60 mm μ_Δ=1	800	1074	3218	1828	1202
x=0.0 m, s=60 mm μ_Δ=4.75	800	1074	2647	1451	1202

x is the distance from the base of the pier to the reference section.
* the shear capacity from tests corresponds to the ultimate capacity at maximum ductility.
# the shear capacity is computed following the provisions of EN1992-1-1

It is also interesting to note that the expressions proposed by EN1998-2 [CEN, 2005] and CSA [2004] lead to similar results at the critical section of the base, in spite of the large differences between the terms accounted by these expressions. The results obtained from this analysis and the large scatter obtained between the expressions proposed, suggests that if any, EN1998-2 [CEN, 2005] gives the most conservative estimate of shear strength, and thus gives a larger margin of safety against failure in shear, which for design purposes, can be considered as beneficial. Nonetheless, research most continue in order to determine with more accuracy the range of validity of these expressions, especially when the effects of factors such as axial force, shear-to-span ratio and ductility demand are taken into account when performing assessment of the shear strength of a reinforced concrete bridge pier.

REFERENCES

American Association of State Highway and Transportation Officials [2004] *AASHTO LRFD bridge design specifications and commentary*, Washington, D.C, U.S.

Ang, B.G., Priesley, M.J.N., Paulay, T. [1989] "Seismic shear strength and deformability of RC bridge columns subjected to inelastic cyclic displacements", *Rep. No. UCB/EERC-92/04*, Earthquake Engineering Research Center, University of California at Berkeley, Berkeley, CA, U.S.

Ang, B.G., Priestley, M.J.N., Paulay, T. [1989] "Seismic shear strength of circular reinforced concrete columns", *ACI Structural Journal*, Vol. 86, No. 1, pp. 45-59.

Applied Technology Council [1983] Seismic retrofitting guidelines for highway bridges, ATC 6-2, Redwood City, CA, U.S.

ASCE-ACI Committee 445 on shear and torsion [1998] "Recent Approaches to shear design of structural concrete", *Journal of Structural Engineering*, ASCE, Vol. 124, No. 12, pp. 1375-1417.

ATC [1996] "Seismic evaluation and retrofit of concrete buildings", Volume 1, ATC-40 Report, Applied Technology Council, Redwood City, California.

ATC [2005] "Improvement of nonlinear static seismic analysis procedures", FEMA 440 Report, Applied Technology Council, Redwood City, California.

Ayala, G. [2001] "Evaluation of the seismic performance of structures: A new approach", (In Spanish), Revista Internacional de Métodos Numéricos para Cálculo y Diseño en Ingeniería, Vol. 17, pp. 285-303.

Ayala G., Paulotto C., Taucer F. [2007] "Evaluation of Iterative DBD procedures for bridges", *EUR Report*, European Laboratory of Structural Assessment, Joint Research Centre, European Commission, Ispra, Italy.

Aydinoğlu, M.N. [2003] "An incremental response spectrum analysis procedure based on inelastic spectral displacements for multi-mode seismic performance evaluation", *Bulletin of Earthquake Engineering*, Vol. 1, No. 1, pp. 3-36.

Bentz, E.C. [2000] "Sectional analysis of reinforced concrete member" *PhD Thesis*, Department of Civil Engineering, University of Toronto, Canada.

Bhide, S.B., Collins, M.P. [1989] "Influence of axial tension on the shear capacity of reinforced concrete members", *ACI Structural Journal*, Vol. 86, No. 5, pp. 570-581.

Blandon, C.A., Priestley, M.J.N. [2005] "Equivalent viscous damping equations for direct displacement-based design", *Journal of Earthquake Engineering*, Vol. 9, No. 2, pp. 257-278.

Calvi, G.M., Kingsley, G.R. [1995] "Displacement Based Seismic Design of Multi-Degree of Freedom Bridge Structures", *Earthquake Engineering and Structural Dynamics*, Vol. 24, No. 9, pp. 1247-1266.

CEN [2003] "Eurocode 8. Design of structures for earthquake resistance – Part 1: General Rules, seismic actions and rules for buildings", Final Draft prEN 1998-1, Commission of the European Communities, Brussels, Belgium.

Chopra A.K., Goel R.K. [2002] "A modal pushover analysis procedure for estimating seismic demands for buildings", *Earthquake Engineering and Structural Dynamics*, Vol. 31, pp. 561-582.

Collins, M.P., Mitchell, D. [1991] *Prestressed concrete structures*, Prentice Hall, Englewood Cliffs, New Jersey, U.S.

Comité Euro-International du Beton (CEB) [1978] *Shear and torsion, June: Explanatory and viewpoint papers on Model Code Chapter 11 and 12*, prepared by CEB Committee V, CEB Bull. 12, Paris, France.

Comité Européen de Normalisation (CEN) [2003] *prEN 1992-1-1 Eurocode 2: Design of concrete structures for earthquake resistence - Part 1-1: General rules and rules for building*, Final Draft, Brussels, Belgium.

Comité Européen de Normalisation (CEN) [2003] *prEN 1998-1 Eurocode 8: Design of structures for earthquake resistence - Part 1: General rules, seismic actions and rules for building*, Final Draft, Brussels, Belgium.

Comité Européen de Normalisation (CEN) [2003] *prEN 1998-2 Eurocode 8: Design of structures for earthquake resistence Part 2: Bridges*, Draft Document TC250/SC8/N370, Brussels, Belgium.

CSA Committee A23.3 [2004] *Design of concrete structures: structures (design) – A national standard of Canada*, Canadian Standards Association, Rexdale, Canada.

De Rue G.M. [1998] "Non-linear Static Procedure Analysis of 3D Structures for Design Applications". *MSc Thesis*, New York State University at Buffalo, USA.

Dwairi, H.M. [2004] "Equivalent Damping in Support of Direct Displacement-Based Design with Applications to Multi-Span Bridges", PhD thesis, Department of Civil, Construction and Environmental Engineering, North Carolina University, Raleigh, N.C.

Fajfar, P. [1999] "Capacity Spectrum Method Based on Inelastic Spectra," *Earthquake Engineering and Structural Dynamics*, Vol. 28, pp. 979-993.

FEMA [1997] "NEHRP Guidelines for the Seismic Rehabilitation of Buildings", FEMA 273; Federal Emergency Management Agency, Washington, D.C.

Freeman, S.A. [1978] "Prediction of Response of Concrete Buildings to Severe Earthquake Motion," *Publication SP-55*, American Concrete Institute, Detroit, MI, pp. 589- 605.

Gulkan, P., Sozen M.A. [1974] "Inelastic responses of reinforced concrete structures to earthquakes motions", *Proceedings of the ACI*, Vol. 71, No. 12, pp. 604-610.

Gupta B, Kunnath S.K. [2000] "Adaptive spectra-based pushover procedure for seismic evaluation of structures. *Earthquake Spectra,* Vol. 16, pp. 367-392.

Guyader C., Iwan W.D. [2006] "Determining equivalent linear parameters for use in a capacity spectrum method of analysis", *Journal of Structural Engineering*, Vol. 132, No. 1, pp. 59-67.

Isaković T.A., Fischinger M. [2006] "Higher modes in simplified inelastic seismic analysis of single column bent viaducts", *Earthquake Engineering and Structural Dynamics,* Vol.. 35, No. 1, pp. 95-114.

Izzudin, B.A., Elnashai, A.S. [1989] "ADAPTIC: A program for adaptive large displacement inelastic analysis of frames" *Engineering Seismology and Earthquake Engineering Rep. No. ESEE 7/89*, Imperial College, London, UK.

Jacobsen, L.S. [1930] "Steady forced vibrations as influenced by damping", *ASME Trans.*, 52, pp. 169-181.

Jacobsen L.S. [1960] "Damping in composite structures", *Proceedings of the 2nd world conference on earthquake engineering*, Tokyo, Japan, Vol. 2, pp. 1029-1044.

Kowalsky, M.J. [2002] "A displacement-based approach for the seismic design of continuous concrete bridges", *Earthquake Engineering and Structural Dynamics*, Vol. 31, pp.719–747.

Kowalsky, M.J, Priestley M.J.N., MacRae G.A. [1995] "Displacement-based design of RC bridge columns in seismic regions", *Earthquake Engineering and Structural Dynamics*, Vol. 24, No. 12, pp. 1623-1643.

Lehman, D.E., Lynn, A.C., Aschleim, M.A., Moehle, J.P. [1996] "Evaluation methods for reinforced concrete columns and connections", *Proceedings of 11th World Conference on Earthquake Engineering*, Paper No. 673, Mexico.

Manfredi, G., Pecce, M. [1998] "Effectiveness of the plastic hinge length in the assessment of the rotation capacity of R.C. columns", *Proc. 11th European Conference on Earthquake Engineering*, pp. 1-11, Paris, France.

Marti, P. (1985) "Truss models in detailing", *Concrete International*, Vol. 7, No. 12, pp. 66-73

Moehle, J.P. [1992] "Displacement based design of RC structures subjected to earthquakes", *Earthquake Spectra*, Vol. 8, No. 3, pp. 403-428.

Mörsch [1909] *Concrete-Steel Construction (Der Eisenbetonbau)*, English translation of the 3rd German edition, McGraw-Hill Book Co., New York, U.S.

Mörsch, E. [1922] *Der Eisenbetonbau-seine theorie und anwendung*, 5th Ed., Vol. 1, Part 2., Wittwer, Stuttgart, Germany.

MTO, OHBDC Committee [1991] *Ontario Highway Bridge Design Code*, 3rd Edition, Ontario Ministry of Transportation Officials, Downsview, Canada.

Norwegian Council for Building Standardization [1992] *Norwegian Standard NS 3473 E*, Norwey.

Palermo, D., Vecchio, F.J. [2003] "Compression field modelling of reinforced concrete subjected to reversed loading: formulation", *ACI Structural Journal*, Vol. 100, No. 5, pp. 616-625.

Paret T.F, Sasaki K.K, Eilbeck D.H, Freeman S.A. [1996] "Approximate inelastic procedures to identify failure mechanisms from higher mode effects", *Proceedings of the 11th World Conference in Earthquake Engineering*, Acapulco, Mexico, Paper 966.

Paulotto, C., Ayala, G., Taucer, F. [2007] "Estimation of equivalent properties for the DBD of rectangular hollow RC bridge piers", *EUR Report*, European Commission, JRC, Ispra (to appear).

Pinto, A.V., Verzelletti, G., Negro, P., Guedes, J. [1995] *Cyclic testing of a squat bridge-pier - Report EUR 16247 EN*, Joint Research Center, European Commission, Ispra, Italy.

Pinto A.V., Verzeletti G., Pegon P. Magonette G., Negro P., Guedes J. [1996] "Pseudo-Dynamic Testing of Lange Scale R/C Bridges", *Report EUR 16378 EN*, European Laboratory for Structural Assessment, Joint Research Centre, European Commission.

Priestley, M.J.N., Park, R. [1987] "Srength and ductility of concrete bridge under seismic loading", *ACI Structural Journal*, Title no. 84-S8, pp. 61-76.

Priestley M.J.N [1993] "Myths and Fallacies in Earthquake Engineering - Conflicts Between Design and Reality", *Proceedings of the Tom Paulay Symposium - Recent Developments in Lateral Force Transfer in Buildings*, San Diego, CA, pp. 229-252.

Priestley, M.J.N., Verma, R., Xiao, Y. [1994] "Seismic shear strength of reinforced concrete columns", *Journal of Structural Engineering*, ASCE, Vol. 120, No. 8, pp. 2310-2239

Priestley, M.J.N., Seible, F., Calvi, G.M. [1996] *Seismic Design and retrofit of bridges*, John Wiley & Sons, New York, U.S., ISBN 0-471-57998-X.

Priestley M.J.N. [2000] "Performance Based Seismic Design", *Proceedings of the 12th World Conference on Earthquake Engineering*, Auckland, NZ. Paper 2831.

Ramirez, J.A., Breen, J.E. [1991] "Evaluation of a modified truss-model approach for beam in shear", *Struct. J. Am. Concrete Inst.*, Vol. 88, No. 5, pp. 562-571.

Requena, M., Ayala, A.G. [2000] "Evaluation of a simplified method for the determination of the nonlinear seismic response of RC frames", *Proceedings of the 12th World Conference on Earthquake Engineering*, Auckland, NZ., Paper 2109.

Ritter, W. [1899] "Die Bauweise Hennebique", *Schweizerische Bauzeitung*, Zürich, Switzerland.

Rosenblueth, E. and Herrera, I., [1964] "On a kind of hysteretic damping", *Journal of the Engineering Mechanics Division*, ASCE, Vol. 90, pp. 37−48.

Ruiz-Garcia, J., Miranda, E. [2004] "Inelastic displacement ratios for design of structures on soft soil sites", *Journal of Structural Engineering*, Vol. 130, No. 12, pp. 2051-2061.

Seneviratna, G.D.P.K., Krawinkler, H. [1997] "Evaluation of inelastic MDOF effects for seismic design. John A. Blume Earthquake Engineering Center, Report No. 120, Department of Civil Engineering, Stanford University.

Schläich, J., Schafer, K., Jennewein, M. [1987] "Toward a consistent design of structural concrete", *Precast/Prestressed Concrete Institute Journal*, Vol. 32, No. 3, pp. 74-150.

Sezen, H., Moehle, J.P. [2004] "Shear Strength Model for Lightly Reinforced Concrete Columns", *Journal of Structural Engineering*, ASCE, Vol. 130, No. 11, pp. 1692-1703.

Shibata, A., Sozen M.A. [1976] "Substitute-Structure Method for Seismic Design in R/C". *Journal of the Structural Division,* ASCE, Vol. 102, No. ST1, pp. 1-18.

Vecchio, F.J. [1989] "Towards cyclic load modelling of reinforced concrete", *ACI Structural Journal*, Vol. 96, No. 2, pp. 132-202.

Veletsos, A., Newmark, N. [1960] "Effect of the inelastic behaviour on the response of simple systems to earthquake motions." *Proceedings of 2nd World Conference on Earthquake Engineering*, Tokyo, Japan, Vol. 2, pp. 895-912.

Vecchio, F.J., Collins, M.P. [1986] "The modified compression-field theory for reinforced concrete elements subjected to shear", *ACI Journal*, Vol. 83, No. 2, pp. 219-231.

Wong, Y.L., Paulay, T., Priestley, M.J.N. [1993] "Response of circular reinforced concrete columns to multi-directional seismic attack", *ACI Structural Journal*, Vol. 90, No. 2, pp. 180-191.

European Commission

EUR 22894 EN – Joint Research Centre – Institute for the Protection and Security of the Citizen
Title: Simplified models/procedures for estimation of secant-to-yielding stiffness, equivalent damping, ultimate deformations and shear capacity of bridge piers on the basis of numerical analysis
Author(s): Carlo PAULOTTO, Gustavo AYALA, Fabio TAUCER, Artur PINTO
Luxembourg: Office for Official Publications of the European Communities
2007 – 52 pp. – 21 x 29.7 cm
EUR – Scientific and Technical Research series – ISSN 1018-5593

Abstract
This report is the result of the contribution of the JRC towards the LESSLOSS Final Report on "Guidelines for Displacement-based Design of Buildings and ", edited by M. N. Fardis and printed by the IUSS Press of the Istituto Universitario Superiore di Pavia. The report is divided into three sections. The first section focuses on the aims and limitations of current seismic evaluation and design practice and the tendencies of the displacement-based seismic evaluation/design methods. The second section presents the secant stiffness and equivalent viscous damping properties of reinforced concrete hollow rectangular bridge piers, both evaluated at maximum pier displacement, while the third section addresses how to determine the deformability or stiffness of bridge piers resulting from the relative contributions of flexural and shear deformations.

The mission of the JRC is to provide customer-driven scientific and technical support for the conception, development, implementation and monitoring of EU policies. As a service of the European Commission, the JRC functions as a reference centre of science and technology for the Union. Close to the policy-making process, it serves the common interest of the Member States, while being independent of special interests, whether private or national.